https://doi.org/10.5194/bg-2021-353
Preprint. Discussion started: 12 January 2022

Biogeosciences Discussions

Genetic functional potential displays minor importance in explaining spatial variability of methane fluxes within a *Eriophorum vaginatum* dominated Swedish peatland.

Joel D. White [a, *], Lena Ström [a], Veiko Lehsten [a,c], Janne Rinne [a,d], Dag Ahrén [b]

[a] Department of Physical Geography and Ecosystem Science, Lund University, Sölvegatan 12 S-223 62 Lund, Sweden. joel.white@nateko.lu.se; lena.strom@nateko.lu.se; veiko.lehsten@nateko.lu.se; janne.rinne@nateko.lu.se

[b] National Bioinformatics Infrastructure Sweden (NBIS), Department of Biology, Sölvegatan 35 Lund University, 22362 Lund, Sweden. dag.ahen@biol.lu.se

[c] Swiss Federal Institute for Forest, Snow and Landscape research (WSL), Birmensdorf, Switzerland.

[d] Natural Resources Institute Finland, Production Systems, Latokartanonkaari 9, 00790 Helsinki, Finland

Correspondence: Joel D. White (joel.white@nateko.lu.se)

https://doi.org/10.5194/bg-2021-353
Preprint. Discussion started: 12 January 2022

Biogeosciences Discussions

Abstract. Microbial communities of methane (CH_4) producing methanogens and consuming methanotrophs play an important role for Earth's atmospheric CH_4 budget. Despite their global significance, knowledge on how much they control the spatial variation in CH_4 fluxes from peatlands is poorly understood. We studied variation in CH_4 producing and consuming communities in a natural peatland dominated by *Eriophorum vaginatum*, via a metagenomics approach using custom designed hybridization-based oligonucleotide probes to focus on taxa and functions associated with methane cycling. We hypothesized that sites with different magnitudes of methane flux are occupied by structurally and functionally different microbial communities, despite the dominance of a single vascular plant species. To investigate this, nine plant-peat mesocosms dominated by the sedge *Eriophorum vaginatum*, with varying vegetation coverage, were collected from a temperate natural wetland and subjected to a simulated growing season. During the simulated growing season, measurements of CH_4 emission, carbon dioxide (CO_2) exchange and $\delta^{13}C$ signature of emitted CH_4 were made. Mesocosms 1 through 9 were classified into three categories according to the magnitude of CH_4 flux. Gross primary production and ecosystem respiration followed the same pattern as CH_4 fluxes, but this trend was not observed in net ecosystem exchange. We observed that genetic functional potential was of minor importance in explaining spatial variability of CH_4 fluxes with only small shifts in taxonomic community and functional genes. In addition, a higher β-diversity was observed in samples with high CH_4 emission. Among methanogens, *Methanoregula*, made up over 50% of the community composition. This, in combination with the remaining hydrogenotrophic methanogens matched the $\delta^{13}C$ isotopic signature of emitted CH_4. However, the presence of acetoclastic and methylotrophic taxa and type I, II and *Verrucomicrobia* methanotrophs indicates that the microbial community holds the ability to produce and consume CH_4 in multiple ways. This is important in terms of future climate scenarios, where peatlands are expected to alter in nutrient status, hydrology, and peat biochemistry. Due to the high functional potential, we expect the community to be highly adaptive to future climate scenarios.

https://doi.org/10.5194/bg-2021-353
Preprint. Discussion started: 12 January 2022

1.0 Introduction

Methane (CH_4) is second most important long-lived greenhouse has in the atmosphere (Dean et al., 2018; Dlugokencky et al., 2009; Saunois et al., 2020). Atmospheric CH_4 concentrations have increased twofold during the industrial period (Dlugokencky et al., 2003). Following a decade of near-zero increase by the turn of the millennium, globally averaged atmospheric CH_4 is on the rise again at a rate of 5 ppb yr^{-1} (Dlugokencky et al., 2009; Dlugokencky et al., 2003; Saunois et al., 2016b; Saunois et al., 2020). CH_4 is emitted from both natural and anthropogenic sources (Dean et al., 2018; Saunois et al., 2016a). Within all natural sources, the largest contributor to CH_4 emissions are wetlands producing 149Tg (range 102–182) CH_4 yr^{-1}, i.e. 40 % of the total natural CH_4 emission (Dean et al., 2018; Saunois et al., 2020).

Microbial CH_4 emission is a byproduct of microbial metabolism and is produced by methanogenic *Archaea* following hydrolysis and fermentation (Ferry, 1999). CH_4 production occurs under anoxic conditions, where organic carbon bound to dead organic matter is converted into CH_4 via methanogenesis (Ferry, 1999). Methanogenesis is the final reaction in anaerobic degradation of organic matter and occurs stepwise in cooperation between different microbial functional groups.

Methanotrophs, of the phyla, *Proteobacteria*, *Verrucomicrobia*, and candidate phylum NC10 act as a natural bio-filter by oxidizing CH_4 and thereby reducing emissions. Inhabiting the oxic-anoxic interfaces, methanotrophs oxidize between 10 to 90% of the CH_4 produced by methanogenic archaea before it is emitted to the atmosphere (Hakobyan and Liesack, 2020; Wendlandt et al., 2010). Methanotrophs can be found in a number of environments including wetlands, marine or freshwater sediments, rice paddies and sewage, and grow on one-carbon compounds such as methanol and methylated amines (Wendlandt et al., 2010; Chen et al., 2008; Dedysh, 2002, 2009). A common characteristic of all aerobic methanotrophs is their ability to oxidize CH_4 to carbon dioxide (CO_2) and water.

CH_4 emissions from natural wetlands are known to exhibit both spatial and temporal variability (Crill et al., 1988; Sun et al., 2013). The spatial variability makes wetland CH_4 emissions difficult to model and predict (Wania et al., 2009, 2010), as CH_4 emission within similar environmental conditions (i.e. ecotype) can vary by several orders of magnitude without an apparent explanation (Bridgham et al., 2013). According to current knowledge, both production and consumption of CH_4 within peatland ecotypes is driven by (i) water table depth (WTD), which determines the thickness of oxic and anoxic zones; (ii) plant species composition, which provides substrates and plant mediated transport of CH_4 to the atmosphere; (iii) soil temperature, which affects the rate of microbiological

https://doi.org/10.5194/bg-2021-353
Preprint. Discussion started: 12 January 2022

processes; and (iv) substrate availability for biogeochemical processes such as methanogenesis and methanotrophy (Joabsson et al., 1999; Korrensalo et al., 2018; Mastepanov et al., 2013; Strack et al., 2004; Ström et al., 2015).

Recent advancements in molecular techniques have allowed researchers to explore further drivers affecting the magnitude of CH_4 fluxes (Fierer et al., 2014; Galand et al., 2003; Galand et al., 2002; Juottonen et al., 2008). Shifts within microbial community composition and function, where metabolic processes occur, are expected to contribute to the observed variability of CH_4 fluxes within ecotypes (Bridgham et al., 2013; Dean et al., 2018). Therefore, the ability to include the functional potential of microbial communities as a potential driver of CH_4 fluxes has gained more attention.

The field of environmental genomics has developed rapidly, utilizing the genetic material taken from un-cultured environmental samples to identify accurately the functional gene composition (Ungerer et al., 2008; Ward et al., 2008). Techniques include the establishment of polymerase chain reaction (PCR) based studies, where marker genes are used to evaluate microbial community composition via amplification of regions conserved across species (Brumfield et al., 2020; Lane et al., 1986). The targeting of the marker gene 16S in ribosomal ribonucleic acid (rRNA) that occur in *Bacterial* and *Archaea* genomes has often been recognized as the gold standard in prokaryotic identification (Brumfield et al., 2020; Lane et al., 1986). In CH_4 research, key genes such as methyl coenzyme M reductase (*mcrA*) and methane monooxygenase component A alpha chain (*mmoX*) are often targeted to determine community composition and functional potential (Chroňáková et al., 2019; Freitag et al., 2010; Galand et al., 2005; Liebner et al., 2012). However, recent research has suggested that studying the entire metagenome increases the possibility to predict soil functional potential as opposed to enriching for singular genes (Gravel et al., 2012; Kushwaha et al., 2015; Manoharan et al., 2015).

In order to attain the necessary depth of sequencing coverage required to analyze the functional potential of soil microbial communities, whole metagenomic sequencing is required (Dinsdale et al., 2008; Fierer et al., 2014). Though, even with the constant advancements in sequencing technology, metagenomics studies require large financial and computational resources to obtain the necessary depth of coverage to ensure small microbial communities, including *Archaea*, are detected (Escobar-Zepeda et al., 2015; Pereira-Marques et al., 2019). In response to these limitations, we applied the molecular technique "captured metagenomics", which targets key genes related to the metabolism of both methanogenic *Archaea* and methanotrophic *Bacteria* (Kushwaha et al., 2015; Manoharan et al., 2015).

https://doi.org/10.5194/bg-2021-353
Preprint. Discussion started: 12 January 2022

Captured metagenomics provides an alternative to studying the entire deoxyribonucleic acid (DNA) pool of metagenomic communities (Gasc et al., 2016; Kushwaha et al., 2015; Manoharan et al., 2015). The sequence capture technique hybridizes DNA fragment targets from a metagenomic DNA fragmented pool through the custom set of probes designed via the MetCap pipeline (Kushwaha et al., 2015). This method makes it possible to target thousands of key genes related to methanogen and methanotroph metabolism, while avoiding lengthy lab hours and massive sequencing efforts required of large-scale metagenomic study. In addition, this allows for multiple biological replicates at a reasonable cost per sample (Gasc et al., 2016; Kushwaha et al., 2015; Manoharan et al., 2015).

Here, we address the functional potential impact of CH_4 producing and consuming microbes on the magnitude of CH_4 flux. To determine the functional genetic diversity, we apply captured metagenomics on genes encoding for enzymes related to CH_4 metabolism on nine peat-plant mesocosms dominated by the sedge *Eriophorum vaginatum*. We aim to (1) identify whether the composition of both CH_4 producing and consuming taxa shift in dissimilarity in response to variations in CH_4 flux, (2) determine whether the β-diversity increases with increasing CH_4 emission; and finally, (3) identify whether the $\delta^{13}C$ of emitted CH_4 matches the dominant taxa in samples.

2.0 Methodology

2.1 Site description

To study the functional diversity of a microbial community producing and consuming CH_4, we collected peat-plant mesocosms from Fäjemyr, an ombrotrophic bog located in Skåne, southern Sweden (56°15'53.3"N 13°33'14.1"E). The peatland is classified as an eccentric bog, and is dominated by semi-forested areas alternating between raised hummocks, hollows and moss lawns (Lonnstad and Löfroth, 1994; Lund et al., 2007). Long-term (1961-1990) mean annual temperature and precipitation are 6.2°C and 700mm respectively (Smhi, 2006). The peat depth ranges between 4-5m, while the peat water pH is generally below 4 throughout the entirety of the growing season (Lund et al., 2007).

Vegetation composition at Fäjemyr is diverse including hummocks dominated by dwarf shrubs such as *Calluna vulgaris* and *Erica tetralix*. The moss lawns are carpeted with *Sphagnum*-mosses including *S. magellanicum* and *S. rubellum*, while the raised drier hummocks are dominated by dwarf Scots pine (*Pinus sylvestris*). The dominant sedge species within the site is *Eriophorum vaginatum* (Lonnstad and Löfroth, 1994; Lund et al., 2007).

https://doi.org/10.5194/bg-2021-353
Preprint. Discussion started: 12 January 2022


Biogeosciences Discussions

2.2 Experimental design

A total of 9 cylindrical mesocosms (height: 26 cm, diameter: 27 cm) were collected on the 30th of March, 2017. The mesocosms, numbered M1-M9, were carefully cut from the peatland, transferred directly into plastic containers for transportation to Lund University (82km away) where they were incubated under temperature and light controlled conditions in a growth room. Over the first month we started at 10 ^{o}C and no light, temperature and light levels were gradually increased to allow the mesocosms to adjust and to simulate the onset of the growing season. For the final 4 weeks of the experiment, the conditions in the growth room were kept at 20 °C, 500 µmol PAR m^{-2} s^{-1} and 17 daylight hours (based on sunrise and sunset at Fäjemyr). Due to the effect of heat radiation from the lamps, the temperature varied over the day from 18±0.3 °C when the lamps were off to 23±1 °C when they were on. Additionally, the light level varied (512±42 µmol PAR m^{-2} s^{-1}) somewhat over the surface due to variations in individual lamp efficiency. The mesocosms were rotated bi-weekly to minimize the effect of spatial variations in growth conditions.

All mesocosms were watered daily with deionized water to maintain a constant water table depth at 5 cm below the surface. During the experiment, weekly to bi-weekly (final 3 weeks, n = 6) measurements of CO_2 and CH_4 fluxes were conducted. The $\delta^{13}C$ of emitted CH_4 was measured on three occasions in the final weeks. Upon completion of the experiment, peat samples were removed from the top oxic-anoxic interface (5 cm), bottom (15 cm) and from the peat sticking to the root surface (rhizosphere) for DNA extraction. Resulting in a total of 27 samples peat samples for genomic analysis (each mesocosm n = 3)

2.3 Flux measurements

Flux measurements of CO_2 and CH_4 were made using the static chamber technique (Crill et al., 1988; Livingston and Hutchinson, 1995). For each mesocosm, 6-minute-long measurements in both light and dark conditions were conducted to establish Net Ecosystem Exchange (NEE) and Ecosystem Respiration (R_{eco}). We used a negative sign convention where negative values indicate an uptake of CO_2 from the atmosphere and positive a release. Gross Primary Production (GPP) was calculated according to the relationship GPP = NEE - R_{eco}. Measurements were performed using a transparent 5-liter cylindrical polycarbonate chamber that was covered with a dark hood for R_{eco} measurements. The chamber was equipped with a rubber list to ensure an airtight seal and a fan to circulate air. Both CO_2 and CH_4 concentrations were measured with a LGR Fast Greenhouse Gas analyser (model 911-0010, Los Gatos Research, CA USA). The CO_2 and CH_4 fluxes were calculated via changes in gas concentration

https://doi.org/10.5194/bg-2021-353
Preprint. Discussion started: 12 January 2022

as a function of time using linear fitting over 6-minute measurement periods. Data was corrected for both air pressure, volume of the chamber and ambient air temperature.

2.4 Stable isotope analysis

The CH_4 emission and its $\delta^{13}C$ signature were determined using a cavity ring-down laser absorption spectrometer with the closed chamber technique described above (G2201i, Picarro, Santa Clara, USA). The surface of each peat mesocosm was covered with a transparent cylindrical chamber for 25-30 minutes while the CH_4 mixing ratio and $\delta^{13}C$-CH_4 was recorded with 1 second intervals. Data was averaged into one minute averages. CH_4 emission were calculated using linear fitting, and the $\delta^{13}C$ signature of emitted CH_4 was determined with a Keeling plot intercept approach (Keeling, 1958; Thom et al., 1993). The resulting $\delta^{13}C$-CH_4 values were corrected by adding a constant value of 3.4 ‰, based of comparison with isotopic mass spectrometer.

2.5 Captured metagenomics

2.5.1 Peat samples and DNA extraction

Peat material was collected from three sampling locations within each mesocosm. Samples were taken from the top oxic-anoxic interface (5 cm), bottom (15 cm) and from the root adjacent peat directly attached to the root surface (10 cm). The peat material was stored at 20°C and then thawed at 4°C prior to DNA extraction. DNA was extracted following the DNeasy® PowerSoil® Kit (Qiagen, Hilden, Germany) and carried out according to the manufacturer's protocol, following the recommended 0.25 g of input material. After DNA extraction, samples were tested for quality (absorbance ratio 260/280) and concentration on a NanoDrop lite (NanoDrop Technologies, Willington NC, USA) and Invitrogen Qubit 4 fluorometer (Thermo Fisher Scientific, Waltham MA, USA) respectively.

2.5.2 SeqCap EZ probe generation

Genes encoding enzymes closely related to the CH_4 production and oxidation in pathway map00680 were identified from the Kyoto Encyclopedia of Genes and Genomes (KEGG). The nucleotide sequences were downloaded via a custom R script (https://github.com/dagahren/metagenomic-project). In total, 548,104 genes were downloaded and compiled into a local database, subsequently referred to here as the CH_4 database. The nucleotide coding sequences of the CH_4 database were used to design hybridisation-based probes for sequence capture. The probe sequences were generated using the MetCap pipeline, where sequences were clustered with

https://doi.org/10.5194/bg-2021-353
Preprint. Discussion started: 12 January 2022

90% sequence similarity with an average of 4 probes per cluster (Kushwaha et al., 2015; Manoharan et al., 2015). In total, 193,386 individual probes were generated after clustering. They were generated with a melting temperature of 55°C and probe length 40mer which is suitable for use with our protocol that is based on NimbleGen SeqCap EZ (Roche NimbleGen Inc., Madison, USA).

2.5.3 Probe hybridisation, library generation and sequencing

Depending on the extracted DNA concentration, 150 ng or 1 µg of genomic DNA in a total volume of 100 µl low TE, was sheared for 13 cycles of 30s on, 30 s off, using a Bioruptor Pico and 0.65 ml Bioruptor tubes (Diagenode SA, Seraing, Belgium). 1 µl of the sheared samples was run on a DNA HS chip prior to contamination clean up. The fragmented DNA was then purified using 1.8× AMPure XP beads (Beckman Coulter, Indianapolis, USA) and used as input material for preparation of pre-capture libraries and constructed according to the Nimblegen SeqCap EZ HyperCap Workflow User's Guide (Version 1.0, June 2016). We used two modifications to this method to allow for improved hybridization: (i) for the adapter ligation step, 5 µl of 15 µM KAPA unique dual index mixed adapters were used instead of single index adapters, (ii) for the pre-capture PCR, 7 cycles was used for libraries with a genomic DNA input of 150 ng, and 5 cycles where the input was 1 µg.

Pre-capture libraries were purified with 1.8x Ampure beads and quantified by Quant-iT double-stranded DNA high sensitivity assay and the average fragment size determined by analysis on a Fragment Analyser (Agilent, Santa Clara, USA) using a high sensitivity NGS Kit. Libraries were multiplexed in pools of 15 in equimolar amounts based on the aforementioned concentrations and sizes. 1 µg of each pool was transferred to a test tube and hybridised to custom probes according to the NimbleGen SeqCap EZ SR User's Guide (Version 4.3, October 2014). When setting up the hybridisations, SeqCap EZ Developer Reagent and HyperCap Universal Blocking Oligos were added to each pool, according to manufacturer's instructions. The capture tubes were incubated in a thermal cycler set at 47 ºC, with the heated lid set to 57 ºC for 69 hours.

The final captured library pool was reagent-treated and further purified using 1.8× AMPure XP beads to remove unligated adapters. The quantity and quality of the final pool was assessed by Qubit and Bioanalyzer and subsequently by qPCR using the Illumina Library Quantification Kit from Kapa on a Roche Light Cycler (LC480II, Basel, Switzerland). Briefly, a 20 µl PCR reaction (performed in triplicate for each pooled library) was prepared on ice with 12 µl SYBR Green I Master Mix and 4 µl diluted pooled DNA (1:1000 to 1:100,000 depending on the initial concentration determined by the Qubit). PCR thermal cycling conditions consisted of

https://doi.org/10.5194/bg-2021-353
Preprint. Discussion started: 12 January 2022

initial denaturation at 95°C for 5 minutes, 35 cycles of 95°C for 30 seconds (denaturation) and 60°C for 45 s for annealing and extension, a melt curve analysis at 95°C and cooling at 37°C.

The captured libraries were sequenced on an Illumina HiSeq4000 platform using sequencing by synthesis technology to generate 2 x 150 base pair (bp) paired-end reads, the analysis was carried out by the Centre for Genomic Research, University of Liverpool, United Kingdom.

2.6 Data Analysis

Raw fastq files were trimmed for the presence of Illumina adapter sequences using Cutadapt version1.2.1 (Martin, 2011). The option -O 3 was used, which means that the 3' end of any reads that matched the adapter sequence were removed by 3bp. The reads were further trimmed using Sickle version 1.200 with a minimum window quality score of 20 (Joshi, 2011). This meant that reads shorter than 20bp were removed.

Following sequence trimming, reads from each of the captured data sets were submitted to Metagenomic Rapid Annotations using Subsystems Technology (MG-RAST) for sequence annotation (Meyer et al., 2008). Default parameters were used for quality filtering of bad reads and removal of sequence duplicates. Once annotated, sequences were filtered for both taxonomic and functional annotations via the KEGG CH_4 metabolism filter (ko:00680). The taxonomic and functional annotations from MG-RAST were annotated using refseq and KEGG (KO) databases (Kanehisa et al., 2015; O'leary et al., 2016). and exported to R for downstream analysis.

2.7 Statistical analysis

All statistics were completed in R and visualized using 'ggplot2' (Hadley, 2016). Given the small sample size (n = 9), as well as the non-normal distribution of the values, a permutation test was used based around the 6 temporal replicates (M1-9 n = 6, total n = 54) of CH_4 and CO_2 flux from each mesocosm and we used an 'independence test' in R from the 'coin' package (Hothorn et al., 2021). We tested pairwise for differences in means and performed a subsequent correction for multiple testing as described by Holm (1979). To evaluate the statistical relationship between CH_4 and CO_2 flux, a Pearson's correlation test was used from the package 'corrplot' (Wei and Simko, 2017).

Further statistical tests for use on genomic data, including the Permutational multivariate analysis of variance (PERMANOVA), α-diversity and β-diversity, and Nonmetric Multidimensional Scaling (NMDS), were completed using the 'vegan' package (Oksanen et al., 2019). Due to the low number of replicates and non-normal

https://doi.org/10.5194/bg-2021-353
Preprint. Discussion started: 12 January 2022

distribution we performed a PERMANOVA to determine the most influential taxa and functional genes (Anderson, 2001). Input data for the PERMANOVA was double root transformed to reduce the influence of highly abundant taxa and genes. When computing the PERMANOVA and NMDS Bray-Curtis distances were used to quantify the compositional dissimilarity between groups with 999 permutations (Anderson, 2001). To test for significance between flux categories, we performed a pairwise comparisons between group levels with False Discovery Rate (FDR) corrections for multiple testing via the 'RVAideMemoire' package (Herv, 2021). Finally, the similarity percentage test (SIMPER) was used to evaluate the contribution of individual taxa and genes to the overall Bray-Curtis dissimilarity, a cut off of 70% was applied (Warton et al., 2012).

3.0 Results

3.1 Mesocosm characteristics

3.1.1 Carbon fluxes

Carbon fluxes of CH_4 and CO_2 vary among the mesocosms and are shown in fig 1. The mean flux of CH_4 mesocosms ranged between 152 (SD ±54) in M9 to 371 (SD ±23) µmol m^{-2} h^{-1} in M4. After observing such large variability within CH_4 fluxes, we performed a pairwise randomization and established that M4 had a significantly higher flux than M1-3 and M5-9 ($p \leq 0.0001$) while M9 had a significantly lower flux ($p \leq 0.0005$) than the remaining mesocosms. For further analysis, we separated the measurements from M4 and M9 from the remaining mesocosms, enabling us to test for a plausible explanation to the observed differences between fluxes when compared to the structure and function of the microbial community. Hereafter, M4 will be referred to as HFM (high flux mesocosm), M9 as LMF (low flux mesocosm) and the remaining mesocosms as MFM (medium flux mesocosm).

GPP and R_{eco} generally followed the same observed pattern as CH_4. With HFM being significantly higher than MFM ($p \leq 0.008$) and LFM ($p \leq 0.004$) in GPP. While R_{eco} was also significantly different between HFM - MFM ($p \leq 0.001$) and HFM - LFM ($p \leq 0.002$). However, the same trend was not observed in NEE, where the highest recorded mean flux was observed in M8 (i.e. MFM category), not in the HFM category as observed in GPP and R_{eco}.

https://doi.org/10.5194/bg-2021-353
Preprint. Discussion started: 12 January 2022

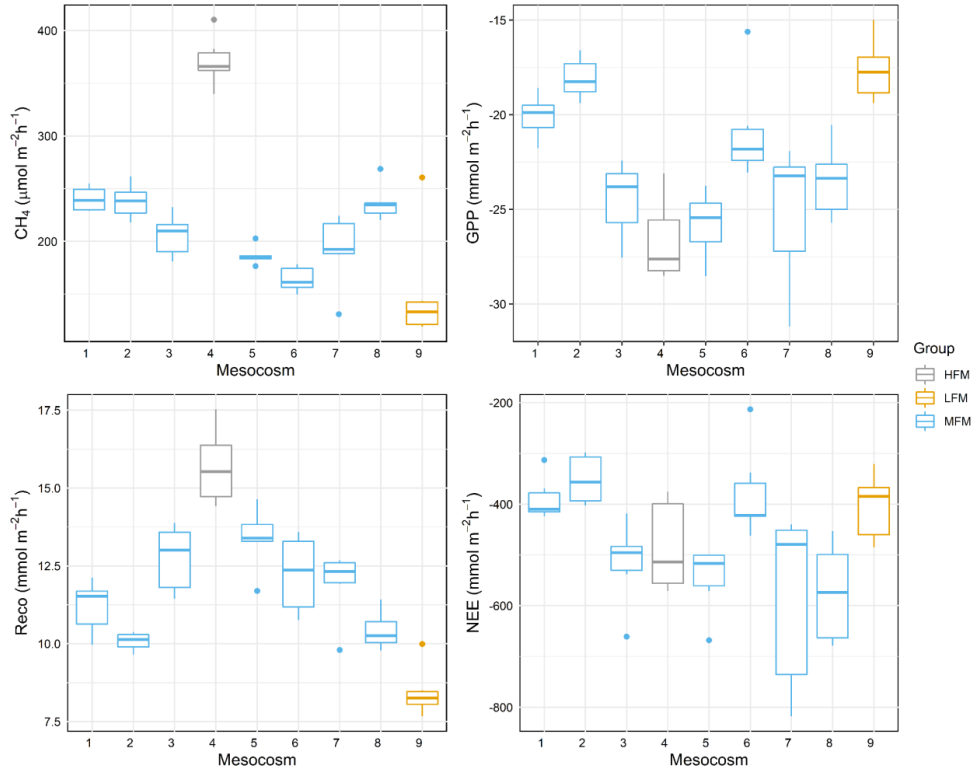

Figure 1: Boxplots of carbon fluxes measured during the last 6 weeks of the lab experiment. The boxes show quartiles and the median, the whiskers denote data within 1.5 times of the interquartile range and the closed circles denote outliers. Methane flux (CH_4), Gross Primary Productivity (GPP), Ecosystem Respiration (R_{eco}), and Net Ecosystem Exchange (NEE). Note the units on the y-axis (mesocosms 1 – 9: n = 6)

In an attempt to investigate the relationships between carbon fluxes we conducted a correlation test and found that the flux of CH_4 held a positive relationship to R_{eco} ($R^2 = 0.60$, $p \leq 0.04$), but not to GPP or NEE (fig 2). When analysing CO_2 fluxes, GPP held a strong negative relationship to R_{eco} ($R^2 = 0.70$, $p \leq 0.002$), while NEE held a strong positive relationship to GPP ($R^2 = 0.82$, $p \leq 0.001$) (fig 2).

3.1.2 Vegetation

The peatland mesocosms were dominated by the sedge *E. vaginatum*, but also included small amounts of the *Sphagnum*-mosses *S. magellanicum* and *S. rubellum*. The number of sedge tillers ranged between 384 in HFM, 276 (mean) in MFM and 134 in LFM (fig 2). The number of *E. vaginatum* tillers held a strong correlation coefficient and significant relationship to GPP ($R^2 = 0.95$, $p \leq 0.01$) and R_{eco} ($R^2 = 0.94$, $p \leq 0.01$) (fig 2). While

https://doi.org/10.5194/bg-2021-353
Preprint. Discussion started: 12 January 2022

279 the remaining carbon fluxes CH_4 (R^2 = 0.44, $p > 0.05$) and NEE (R^2 = 0.64, $p > 0.05$) had a high correlation
280 coefficient, this relationship was not significant to the number of *E. vaginatum* tillers.

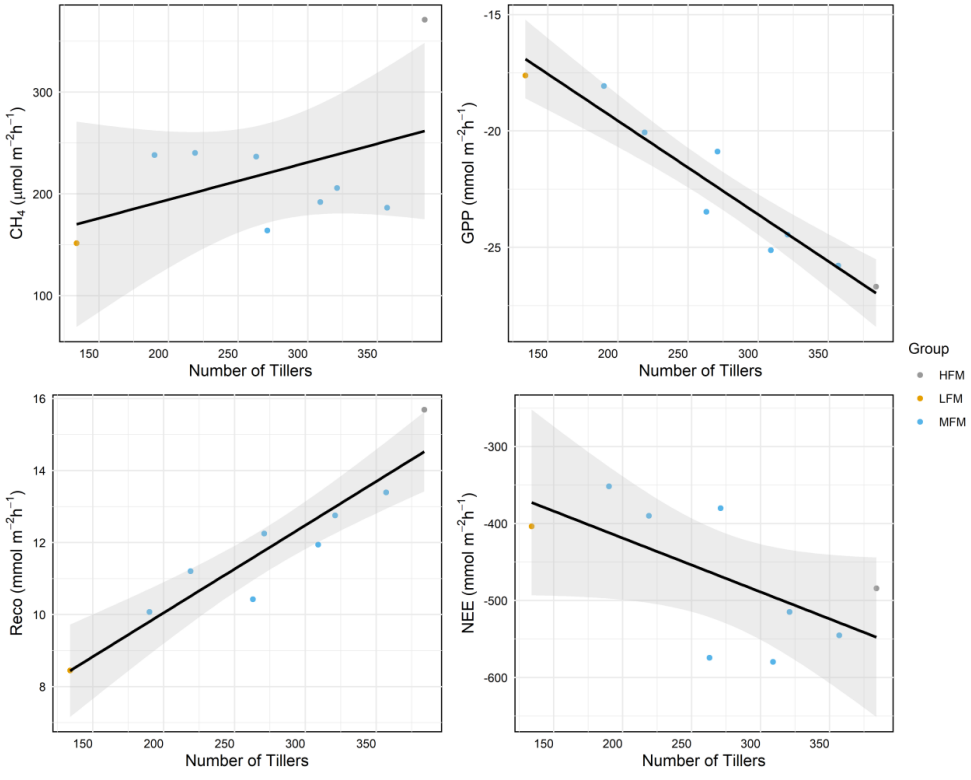

281

282 **Figure 2:** The relationship between mesocosm carbon fluxes and the number of tillers of *E. vaginatum*.
283 Data points represent the mean flux of each individual mesocosm while the shaded area indicates the
284 95% confidence level interval for predictions of the linear model.

285 **3.1.3 Isotopic signature**

286 Distinct isotopic signatures of individual mesocosms are shown in fig 3. All mesocosms fell within the range of
287 hydrogenotrophic methanogenesis ($\delta^{13}C$ = −110‰ to −60‰) (Chanton, 2005; Whiticar, 1999). However, M2
288 (MFM) and M4 (HFM) indicated a slight tendency towards acetoclastic methanogenesis with less negative
289 isotopic signature ($\delta^{13}C$ = -60‰ to -50‰), both yielding mid -60‰ $\delta^{13}C$ Keeling intercepts. A significant positive
290 correlation (R^2 = 0.5, $p \leq 0.001$) and significant relationship also existed between CH_4 flux and the Keeling
291 intercept shown in fig 3.

https://doi.org/10.5194/bg-2021-353
Preprint. Discussion started: 12 January 2022

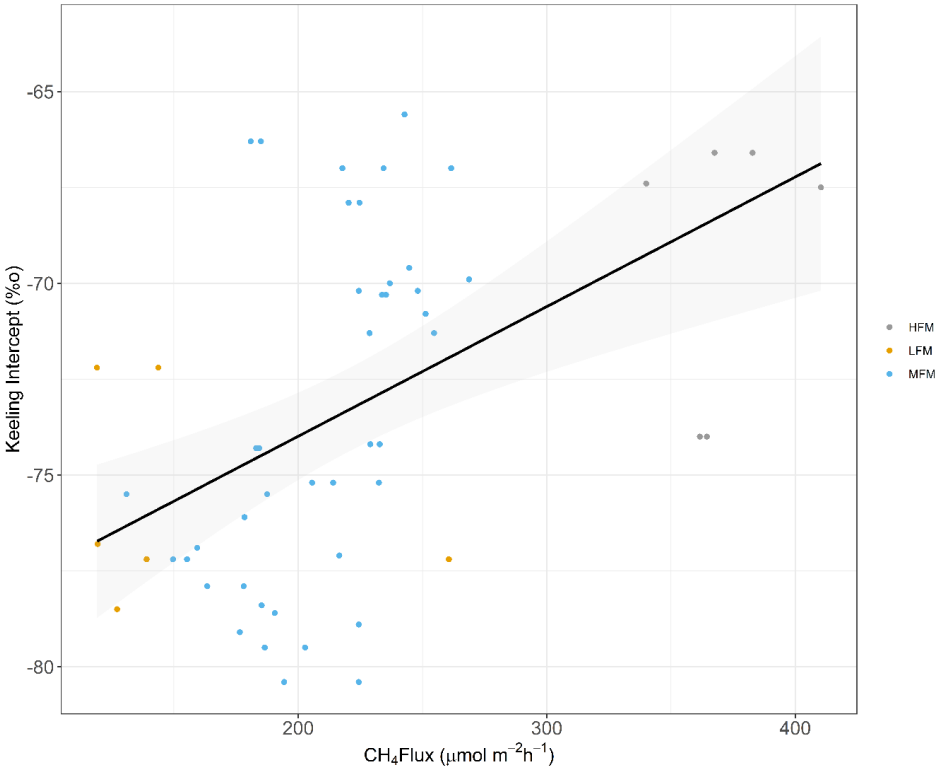

Figure 3: Scatter plot visualizing the relationship between CH_4 flux (µmol m^{-2} h^{-1}) and Isotopic signature of emitted CH_4 (keeling intercept ‰). Data points colored by flux category while the shaded area indicates the 95% confidence level interval for predictions of the linear model.

3.2 Captured Metagenomics

3.2.1 Microbial community composition

Diverse methanogenic *Archaea* and methanotrophic *Bacteria* were observed in all samples. In total, 20 methanogenic *Archaea* and 5 methanotrophic *Bacteria* were detected. Methanogens which utilize CO_2 + H_2, methanol, acetate and methyl amines substrates for ATP and biomass production were all observed throughout the samples, which indicates a high functional potential. Although less diverse than the methanogens, methanotrophs from *Alphaproteobacteria*, *Gammaproteobacteria* and *Verrucomicrobia Phylum* were present in all samples. However, due to the environmental conditions no methanotrophs from the NC10 *Phylum* were detected. This community composition resulted in a median α-diversity measure of 2.38, which is a measure of the diversity of the peatland ecosystem.

https://doi.org/10.5194/bg-2021-353
Preprint. Discussion started: 12 January 2022

306 **3.2.2 Total taxonomic distribution**

307 At genus level, 20 methanogenic genera were identified. The highest relative abundance of methanogens included
308 *Methanoregula* which contributed 54% to the total proportion, followed by *Methanosarcina* (17%),
309 *Methanosphaerula* and *Methanothermobacter* which contributed 5% each to the total proportion of methanogens
310 (fig 2). Within the methanogen community, genera with the ability to metabolize via hydrogenotrophic,
311 acetoclastic and methylotrophic methanogenesis pathways were also detected. Hydrogenotrophic methanogens
312 made up (78%) of the total proportion, while *Methanosarcina* which can utilize several substrates for ATP and
313 biomass production contributed 17%, followed by methylotrophic methanogens (<5%) and finally, acetoclastic
314 methanogens which contributed to <1% of the total.

315 In addition to methanogens, 5 genera of CH_4 reducing *Bacteria* were detected including methanotrophs from
316 *Alphaproteobacteria, Gammaproteobacteria* and *Verrucomicrobia* class. Type II *Alphaproteobacteria* was the
317 dominant *Subphylum*, including both *Methylocella* (37%) which contributed to largest proportion, followed by
318 *Methylosinus* (28%). Type I *Gammaproteobacteria* genera *Methylococcus* (14%) and *Methylobacter* (10%)
319 represented the lowest proportion. Finally, *Verrucomicrobia* included one genus, *Methylacidiphilum*, which
320 contributed to 10% of the total proportion of methanotrophs.

321 **3.2.3 β-diversity**

322 β-diversity, which measures the change in diversity of species from one category to another, was measured as
323 mean distance to the group centroid and highest in HFM (fig 4). HFM resulted in an average distance to median
324 of 0.046, followed by MFM (0.042) and LFM (0.031). The largest distance between medians to centroids was
325 observed between HFM and LFM, while the smallest distance between medians to centroids was observed
326 between MFM and LFM. Due to a high variation and lack of replication, this relationship was observed as non-
327 significant. Although the values for β-diversity are low, the differences between centroids indicates that
328 communities of methanogens and methanotrophs become more similar to each other as the magnitude of flux
329 decreases.

https://doi.org/10.5194/bg-2021-353
Preprint. Discussion started: 12 January 2022

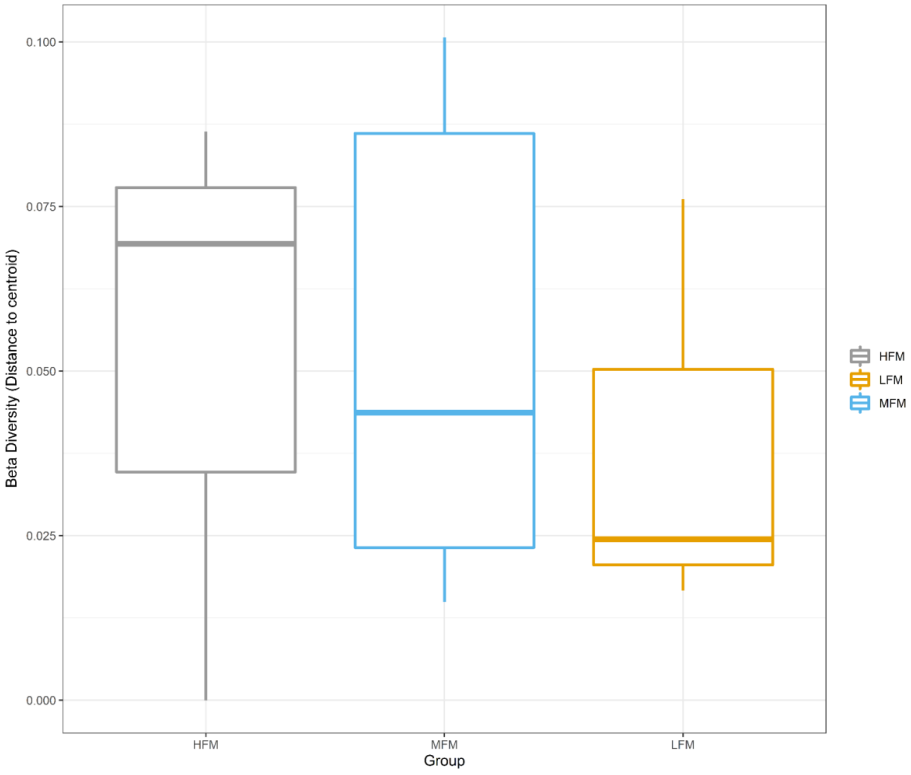

Figure 4: β-diversity boxplot of multivariate homogeneity of groups using Bray-Curtis distances. Dispersions of samples analyzed at genus level across HFM, MFM and LFM (HFM n = 3, MFM n = 21, LFM n = 3).

3.2.4 Taxonomy

The PERMANOVA and SIMPER analysis showed that the variation between the relative abundance of taxa between HFM, MFM and LFM was not significant. The small differences resulted in a non-significant weak correlation where 6% of the variation in taxa could be explained by HFM, MFM or LFM ($R^2 = 0.06$, $p \geq 0.05$). When comparing the relative abundance of methanogens and methanotrophs between HFM, MFM and LFM, five taxa including *Methanoregula*, *Methanosarcina*, *Methylocella*, *Methylosinus* and *Methylobacter* always contributed to the top 70% of cumulative sums (table 1, 2 and 3). However, in the HFM to LFM comparison, the addition of a sixth genus, *Methylacidiphilum*, was required to reach the 70% cut off (Table 3).

In all three comparisons, we observe that the hydrogenotrophic *Methanoregula* contributed the most to dissimilarity (table 1, 2 and 3) while type II *Alphaproteobacteria genera*, *Methylocella* and *Methylosinus*

https://doi.org/10.5194/bg-2021-353
Preprint. Discussion started: 12 January 2022

contributed the second and third highest between flux categories. The order of contributions from the remaining taxa *Methanosarcina*, *Methylobacter* and *Methylacidiphilum* changed depending on the comparison between HFM, MFM and LFM.

Table 1: Results of SIMPER analysis. Taxa are ranked according to their average contribution to dissimilarity between MFM and HFM. Average abundances, ratio (between averages using the greatest common denominator), relative contribution of taxa and *p*-value of the permutation test (Probability of getting a larger or equal average contribution in random permutation of the group factor) are also included. A cut-off at a cumulative dissimilarity of 70% was applied.

Genus	Average	SD	Avg. MFM	Avg. HFM	Ratio	Relative Contribution (%)	p - value
Methanoregula	0.094	0.06	4370	7752	115:204	33%	0.17
Methylocella	0.035	0.02	4826	5842	19:23	12%	0.39
Methylosinus	0.035	0.02	3440	4586	1720:2293	13%	0.21
Methanosarcina	0.019	0.01	1985	2699	1985:2699	7%	0.31
Methylobacter	0.015	0.01	1234	1810	617:905	5%	0.26

Table 2: Results of SIMPER analysis. Taxa are ranked according to their average contribution to dissimilarity between MFM and LFM. Average abundances, ratio (between averages using the greatest common denominator), relative contribution of taxa and *p*-value of the permutation test (Probability of getting a larger or equal average contribution in random permutation of the group factor) are also included. A cut-off at a cumulative dissimilarity of 70% was applied.

Genus	Average	SD	Avg. MFM	Avg. LFM	Ratio	Relative Contribution (%)	p - value
Methanoregula	0.061	0.04	4370	3757	4370:3757	26%	0.91
Methylocella	0.033	0.02	4826	5111	254:269	15%	0.45
Methylosinus	0.032	0.02	3440	4323	3440:4323	14%	0.32
Methylobacter	0.017	0.01	1234	1647	1234:1647	8%	0.10

https://doi.org/10.5194/bg-2021-353
Preprint. Discussion started: 12 January 2022

Methanosarcina	0.015	0.01	1234	1647	1234:1647	7%	0.95

Table 3: Results of SIMPER analysis. Taxa are ranked according to their average contribution to dissimilarity between HFM and LFM. Average abundances, ratio (between averages using the greatest common denominator), relative contribution of taxa and *p*-value of the permutation test (Probability of getting a larger or equal average contribution in random permutation of the group factor) are also included. A cut-off at a cumulative dissimilarity of 70% was applied.

Genus	Average	SD	Avg. HFM	Avg. LFM	Ratio	Relative Contribution (%)	p - value
Methanoregula	0.063	0.07	7752	3757	456:221	26%	0.71
Methylocella	0.035	0.03	5842	5111	5842:5111	15%	0.44
Methylosinus	0.034	0.02	4586	4323	4586:4323	15%	0.32
Methanosarcina	0.017	0.01	2699	1861	2699:1861	7%	0.61
Methylobacter	0.014	0.01	1810	1647	1810:1647	6%	0.47
Methylacidiphilum	0.013	0.008	1880	1290	188:129	6%	0.50

3.2.5 Functional gene composition

Of the total captured gene pool, 64% of sequence annotations were categorized by MG-RAST as coding for metabolism (KO level 1). For metabolism pathways, the top three sub-categories (KO level 2) were distributed across amino acid metabolism (32%), carbohydrate metabolism (27%) and energy metabolism (11%). Within the energy metabolism category, CH_4 metabolism (PATH: KO00680) made up 17% of the captured genes (KO level 4) with a total of 109 genes coding for CH_4 metabolism.

The composition of the functional genes can be observed in the NMDS (fig 5). The NMDS displays the functional genes grouped by HFM, MFM and LFM. Within the NMDS, we observe an overlapping between HFM, MFM and LFM with a lack of distinct separation between clusters, indicating similar abundances and variation within

https://doi.org/10.5194/bg-2021-353
Preprint. Discussion started: 12 January 2022

374 HFM, MFM and LFM. The PERMANOVA also calculated the coefficient of determination and revealed that only
375 7% (R^2 = 0.07, $p \geq 0.44$) of the variation in functional genes can be explained by HFM, MFM and LFM. Finally,
376 we checked for differences between the means of HFM, MFM and LFM via pairwise distances and found no
377 significant difference ($p \geq 0.05$).

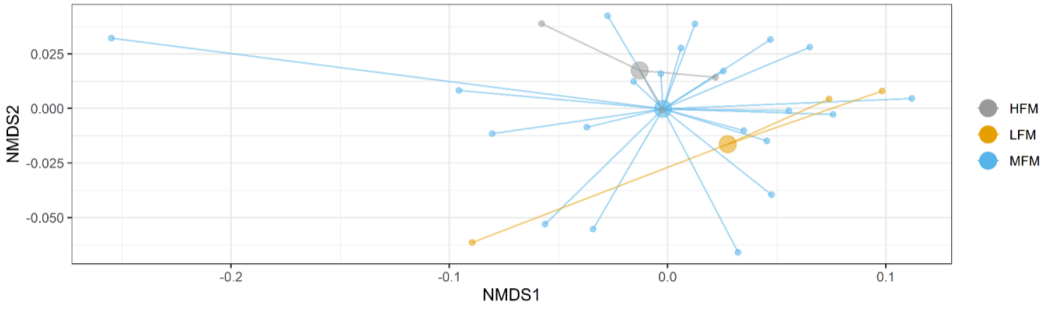

378

379 **Figure 5:** Nonmetric Multidimensional Scaling (NMDS) of functional genes using Bray-Curtis distances.
380 Samples analyzed at KO functional level 4 and colored by HFM, MFM and LFM (HFM n=3, MFM n=21,
381 LFM n=3).

382 In total, 21 genes of the 109 contributed to 70% of the cumulative sum (table 4, 5 and 6). When comparing HFM
383 to MFM and LFM, the Wilks' pairwise post hoc test revealed no significant difference between MFM ($p \geq 0.05$)
384 and LFM ($p \geq 0.05$). Within the two comparisons, we observed that heterodisulfide reductase subunit A (*hdrA*)
385 was the highest cumulative contributor to dissimilarity. In HFM, *hdrA* contributed to 13% of the cumulative total
386 (table 4). When comparing to LFM, *hdrA* contributed 10%, 3% lower than the HFH to MFM comparison (table
387 6). However, the permutation test revealed no significant difference between both MFM and LFM with regards
388 to abundance of *hdrA* (table 4). Within the top 70% of cumulative genes, only the abundance of particulate
389 methane monooxygenase (*pmoA)* was significantly higher in HFM when compared to MFM ($p \leq 0.01$) (table 4).

390 As observed in the HFM comparisons, 21 genes contributed to the total 70% cumulative sum of all captured genes
391 when compared between HFM (table 4) and LFM (table 5). The Wilks' pairwise post hoc test revealed no
392 significant difference between HFM and LFM when compared to MFM (table 5). The largest contributor to the
393 cumulative sum of genes in MFM when compared to HFM and LFM was the *hdrA* gene. The *hdrA* gene
394 contributed to 13% in both comparisons. However, when comparing the abundances of the hdrA gene between
395 HFM and LFM, the decrease was non- significant. However, as identified in the earlier comparison, the abundance

https://doi.org/10.5194/bg-2021-353
Preprint. Discussion started: 12 January 2022

of *pmoA* was significantly lower ($p \leq 0.01$) in HFM when compared to MFM (table 4), but the same observation was not observed when testing abundances in LFM ($p \geq 0.21$) (table 5). Interestingly, *mcrA*, *mcrG* and *mtd* genes were significantly higher in LFM when compared to MFM ($p \leq 0.02$) (table 6).

As with the previous comparisons, 21 genes contributed to the cumulative sum of 70% within the LFM. However, the order and amount contributed to dissimilarity were not the same. The Wilks pairwise post hoc test revealed no significant difference between HFM and MFM when compared to LFM ($p \geq 0.05$). Similarly, the *hdrA* gene was the largest contributor to the cumulative sum in HFM and MFM (table 5 and 6). The largest difference in the abundance of the *hdrA* gene occurred within HFM where the abundance increased by 3% (table 6). However, the increase was identified as non-significant. Interestingly, the *mcrA* gene was highest in abundance in LFM (277), 54% higher than in HFM and 39% higher than MFM.

https://doi.org/10.5194/bg-2021-353
Preprint. Discussion started: 12 January 2022

406 **Table 4:** Results of SIMPER analysis. Genes are ranked according to their average contribution to
407 dissimilarity between MFM and HFM. Average abundances, ratio (between averages using the greatest
408 common denominator), relative contribution of taxa and *p*-value of the permutation test (Probability of
409 getting a larger or equal average contribution in random permutation of the group factor) are also
410 included. A cut-off at a cumulative dissimilarity of 70% was applied.

Contrast: MFM – HFM	Average	SD	Avg. MFM	Avg. HFM	Ratio	Relative Contribution (%)	p - value
hdrA - Heterodisulfide reductase subunit A	0.040	0.044	429	225	143:75	13	0.72
cutL/coxL - Carbon monoxide dehydrogenase large chain	0.026	0.028	525	354	175:118	9	0.28
mcrA - Methyl-coenzyme M reductase subunit A	0.018	0.016	168	126	4:3	6	0.87
coxS - carbon monoxide dehydrogenase small subunit S	0.013	0.012	272	186	136:93	5	0.42
frhG – coenzyme F420 hydrogenase gamma subunit G	0.010	0.009	98	65	98:65	3	0.54
mtrA – tetrahydromethanopterin S methyltransferase subunit A	0.009	0.008	80	80	1:1	3	0.73
mvhA /vhuA /vhcA -F420 non reducing hydrogenase subunit A	0.008	0.008	86	45	86:45	3	0.66
cooS – carbon monoxide dehydrogenase catalytic subunit S	0.008	0.006	91	64	91:64	3	0.76
cutM/coxM – carbon monoxide dehydrogenase medium subunit M	0.007	0.007	145	99	145:99	3	0.42
fwdB/fmdB – formylmethanofuran dehydrogenase subunit B	0.007	0.007	83	59	83:59	2	0.95

https://doi.org/10.5194/bg-2021-353
Preprint. Discussion started: 12 January 2022

metF – methylenetetrahydrofolate reductase NADPH	0.007	0.006	128	81	128:81	3	0.27
pmoA - particulate methane monooxygenase	0.007	0.006	21	62	21:62	2	**0.01**
hoxH - hydrogen dehydrogenase	0.007	0.005	120	84	10:7	2	0.41
mttB – trimethylamine corrinoid protein CO methyltransferase	0.006	0.005	96	63	32:21	2	0.24
mtrH - tetrahydromethanopterin S methyltransferase subunit	0.005	0.004	59	42	59:42	2	0.92
fwdD/fmdD – formylmethanofuran dehydrogenase subunit D	0.004	0.004	38	33	38:33	2	0.76
mtrE - tetrahydromethanopterin S methyltransferase subunit E	0.004	0.004	43	32	43:32	1	0.86
hdrB – heterodisulfide reductase subunit B	0.004	0.003	55	37	55:37	2	0.91
mtrF - tetrahydromethanopterin S methyltransferase subunit F	0.004	0.003	38	25	38:25	1	0.95
mcrG – methyl coenzyme M reductase gamma subunit	0.004	0.003	44	52	11:13	2	0.79
CODH ACSA – carbon monoxide dehydrogenase/acetyl CoA synthase subunit alpha	0.004	0.004	42	20	21:10	1	0.65

411

https://doi.org/10.5194/bg-2021-353
Preprint. Discussion started: 12 January 2022

412 **Table 5:** Results of SIMPER analysis. Genes are ranked according to their average contribution to
413 dissimilarity between MFM and LFM. Average abundances, ratio (between averages using the greatest
414 common denominator), relative contribution of taxa and *p*-value of the permutation test (Probability of
415 getting a larger or equal average contribution in random permutation of the group factor) are also
416 included. A cut-off at a cumulative dissimilarity of 70% was applied.

Contrast: MFM – LFM	Average	SD	Avg. MFM	Avg. LFM	Ratio	Relative Contribution (%)	p – value
hdrA - Heterodisulfide reductase subunit A	0.045	0.034	429	448	429:448	13	0.51
mcrA - Methyl-coenzyme M reductase subunit A	0.027	0.017	168	277	168:277	8	0.15
cutL/coxL - Carbon monoxide dehydrogenase large chain	0.021	0.016	525	573	175:191	6	0.82
fwdB/fmdB – formylmethanofuran dehydrogenase subunit B	0.014	0.009	83	161	83:161	4	0.05
mtrA – tetrahydromethanopterin S methyltransferase subunit A	0.014	0.008	80	143	80:143	4	0.10
coxS - carbon monoxide dehydrogenase small subunit S	0.011	0.007	272	311	272:311	3	0.87
mvhA/vhuA/vhcA -F420 non reducing hydrogenase subunit A	0.010	0.006	86	103	86:103	3	0.39
cooS – carbon monoxide dehydrogenase catalytic subunit S	0.010	0.007	91	125	91:125	3	0.36
frhG – coenzyme F420 hydrogenase gamma subunit G	0.009	0.008	98	113	98:113	3	0.70
mtrH - tetrahydromethanopterin S methyltransferase subunit	0.008	0.005	59	96	59:96	2	0.09
mtrE - tetrahydromethanopterin S methyltransferase subunit E	0.008	0.004	43	85	43:85	3	0.07

https://doi.org/10.5194/bg-2021-353
Preprint. Discussion started: 12 January 2022

mtrF - tetrahydromethanopterin S methyltransferase subunit F	0.007	0.004	38	77	38:77	2	0.05
fwdD/fmdD – formylmethanofuran dehydrogenase subunit D	0.007	0.004	38	76	1:2	2	0.06
mcrG – methyl coenzyme M reductase gamma subunit	0.007	0.004	44	84	11:21	2	**0.02**
hoxH - hydrogen dehydrogenase	0.007	0.005	120	153	40:51	2	0.44
mtd – methylenetetrahydromethanopterin dehydrogenase	0.006	0.004	38	76	1:2	2	**0.02**
cutM/coxM – carbon monoxide dehydrogenase medium subunit	0.006	0.005	145	148	145:148	2	0.85
frhB – coenzyme F420 hydrogenase β- subunit	0.006	0.004	49	80	49:80	2	0.08
metF – methylenetetrahydrofolate reductase NADPH	0.006	0.005	128	156	32:39	1	0.88
hdrB – heterodisulfide reductase subunit B	0.006	0.004	55	82	55:82	2	0.24
mcrB – methyl coenzyme M reductase β- subunit	0.005	0.003	32	63	32:63	2	**0.02**

417

418

https://doi.org/10.5194/bg-2021-353
Preprint. Discussion started: 12 January 2022

Table 6: Results of SIMPER analysis. Genes are ranked according to their average contribution to dissimilarity between HFM and LFM. Average abundances, ratio (between averages using the greatest common denominator), relative contribution of taxa and p-value of the permutation test (Probability of getting a larger or equal average contribution in random permutation of the group factor) are also included. A cut-off at a cumulative dissimilarity of 70% was applied.

Contrast: HFM – LFM	Average	SD	Avg. HFM	Avg. LFM	Ratio	Relative Contribution (%)	p – value
hdrA - Heterodisulfide reductase subunit A	0.040	0.016	225	448	225:448	10	0.65
cutL/coxL - Carbon monoxide dehydrogenase large chain	0.032	0.016	354	573	118:191	8	0.28
mcrA - Methyl-coenzyme M reductase subunit A	0.028	0.012	126	277	126:277	7	0.25
coxS - carbon monoxide dehydrogenase small subunit S	0.017	0.005	186	311	186:311	5	0.20
fwdB/fmdB – formylmethanofuran dehydrogenase subunit B	0.016	0.007	59	161	59:161	4	0.06
mtrA – tetrahydromethanopterin S methyltransferase subunit A	0.015	0.006	80	143	80:143	3	0.13
metF – methylenetetrahydrofolate reductase NADPH	0.011	0.004	81	156	27:52	3	0.06
cooS – carbon monoxide dehydrogenase catalytic subunit S	0.010	0.006	64	125	64:125	3	0.37
mvhA/vhuA/vhcA -F420 non reducing hydrogenase subunit A	0.010	0.005	45	103	45:103	2	0.48
mtrH - tetrahydromethanopterin S methyltransferase subunit	0.009	0.004	42	96	7:16	3	0.09
frhG – coenzyme F420 hydrogenase gamma subunit G	0.009	0.004	65	113	65:113	2	0.59

https://doi.org/10.5194/bg-2021-353
Preprint. Discussion started: 12 January 2022

hoxH - hydrogen dehydrogenase	0.009	0.005	84	153	28:51	2	0.17
mttB – trimethylamine corrinoid protein Co methyltransferase	0.009	0.004	63	126	1:2	3	0.06
mtrF - tetrahydromethanopterin S methyltransferase subunit F	0.008	0.003	25	77	25:77	2	0.05
mtrE - tetrahydromethanopterin S methyltransferase subunit E	0.008	0.004	32	85	32:85	2	0.14
fwdB/fmdB – formylmethanofuran dehydrogenase subunit B	0.008	0.004	33	76	33:76	2	0.09
cutM/coxM – carbon monoxide dehydrogenase medium subunit	0.008	0.007	99	148	99:148	2	0.51
mcrG – methyl coenzyme M reductase gamma subunit	0.008	0.003	52	84	13:21	2	0.05
mtd – methylenetetrahydromethanopterin dehydrogenase	0.007	0.004	31	76	31:76	2	0.05
frhB – coenzyme F420 hydrogenase β- subunit	0.007	0.003	35	80	7:16	1	0.09
hdrB – heterodisulfide reductase subunit B	0.006	0.004	37	82	37:82	2	0.28

424

https://doi.org/10.5194/bg-2021-353
Preprint. Discussion started: 12 January 2022

4.0 Discussion:

4.1 Functional potential of the microbial community

The dominant methane production pathway within our samples, as shown by the taxonomy and $\delta^{13}C$ signal of emitted CH_4, was hydrogenotrophic methanogenesis. However, the presence of the genera acetoclastic *Methanosaeta* and *Methanosarcina*, which possess a more diverse genome allowing them to perform hydrogenotrophic, acetoclastic and methylotrophic methanogenesis, suggests that the community holds a metabolic potential to produce CH_4 under altered environmental conditions. In addition, the presence of type *I*, *II* and *Verrucomicrobia Proteobacteria* indicates that peatland methanotrophs hold the ability to oxidise CH_4 via Ribulose monophosphate, Serine or Calvin-Benson-Bassham cycles. Therefore, if temperate peatland environmental conditions which govern the production and consumption of CH_4 are to change under future climate scenarios, we can expect CH_4 production and consumption to still occur, but possibly using alternative metabolic pathways than currently observed.

The potential to produce and consume CH_4 under alternate environmental conditions is in agreement with other metagenomics studies, which concluded that shifts from one dominant functional group to another can occur as the microbial community already holds the metabolic potential to degrade soil organic carbon via different metabolic pathways (Manoharan et al., 2017; Tveit et al., 2013). The rate of such shifts is dependent upon the delivery of necessary products and environmental conditions conducive for methanogenesis. In the absence of acetogenesis and fermentation, the less dominant functional groups (i.e. acetoclastic and methylotrophic methanogens) may still remain dormant, due to the absence of necessary substrates to metabolize.

4.2 Carbon flux characteristics

We observed a high spatial variability in CH_4 flux, which is consistent with research conducted in other temperate peatlands (Keane et al., 2021; Sun et al., 2013). The same pattern observed in CH_4 fluxes was also detected in GPP and R_{eco}, but not in NEE. The high productivity, observed as high GPP, may be explained by a higher amount of photosynthetic biomass within HFM, than in MFM and LFM. R_{eco} followed the same pattern as CH_4 and GPP, with highest observed flux in HFM and lowest in LFM. One potential reason for the high respiration from HFM could be the significantly higher relative abundance of *pmoA*. The *pmoA* gene codes for the first step in methanotrophy, where CH_4 is reduced to methanol, and finally CO_2, which is often used as a proxy for methanotrophy (Franchini et al., 2015; Freitag et al., 2010). The higher abundance of *pmoA* may indicate a higher

https://doi.org/10.5194/bg-2021-353
Preprint. Discussion started: 12 January 2022

rate of methanotrophy, which may help to explain the higher CO_2 flux respired by the methanotrophs in HFM. In addition, higher plant productivity causes higher autotrophic respiration, which generally makes up ~50% of $R_{eco.}$ However, the vegetation may also be supplying more substrates to the microbial community, which in turn is consumed and respired in the form of CO_2. Characteristics beyond our control, such as redox potential, oxic status and substrate availability, may have additionally contributed to the variability in CH_4 and CO_2 fluxes (Bridgham et al., 2013; Ström et al., 2012).

4.3 The relationship between CH_4 magnitude and functional genes

When comparing the dissimilarity of taxa and functional genes between flux categories, we discovered small dissimilarities in taxonomy and functional genes. This result indicates that, while variation within carbon fluxes is observed, the use of taxa and functional genes only explains a small amount of the variability and hence the relationship is not statistically significant.

4.3.1 Taxonomic

We found that the microbial community had a higher diversity of methanogens than methanotrophs. This can be the result of the high WTD limiting the habitable area of oxic-anoxic interface. The most abundant methanogen, *Methanoregula*, has been frequently detected in ombrotrophic peatland ecosystems and appears to dominate in sites with high *Eriophorum spp*. (Andersen et al., 2013, Chroňáková et al., 2019, Lin et al., 2014, Preston et al., 2012). The tussock building *E. vaginatum* provides a habitable environment for fermenters and syntrophic bacteria where substrates such as H_2 and CO_2 for hydrogenotrophic methanogenesis are most likely more available due to the increase in oxygen provided to the peat through aerenchyma tissue of the plant (Chroňáková et al., 2019; Preston et al., 2012).

When comparing our results to other metagenomic approaches, we find a higher diversity of methanogens than previous research. We identified 20 genera of methanogens, while Lin et al. (2012) detected 16 genera of methanogens using a whole metagenomic approach. We observe slightly higher diversity than studies in other ombrotrophic peatland environments, where sequences belonging to the orders *Methanomicrobiales*, *Methanobacteriales*, and *Methanosarcinales* were detected (Galand et al., 2003; Horn et al., 2003b; He et al., 2015). However, it is difficult to conclude whether our results differ from other studies because of biological factors, different site characteristics or the addition of newly sequenced genomes within the databases used between studies.

https://doi.org/10.5194/bg-2021-353
Preprint. Discussion started: 12 January 2022

The composition of the microbial community was dominated by hydrogenotrophic methanogens. The dominant genus, *Methanoregula*, is recognized as an indicative genus to ombrotrophic peatlands (Andersen et al., 2013; Chroňáková et al., 2019; Lin et al., 2014; Preston et al., 2012), and this is further confirmed by our results. This result was expected as methanogenic communities in ombrotrophic bogs differ significantly compared to fen ecosystems (Horn et al., 2003b). However, the presence of acetoclastic and methylotrophic methanogens within our samples indicates a high functional potential of ombrotrophic bogs with possibilities to switch between dominant methanogenic functional groups. Theoretically, if conditions were to shift within the peatland to favor acetoclastic or methylotrophic methanogenesis, the microbial community holds the functional potential to continue producing CH_4 with little to no delay in transition period. This conclusion is of course made assuming that the necessary substrates and environmental conditions are met.

When comparing the abundances of methanotrophs between HFM, MFM and LFM, we identified that the top 3 contributors to the cumulative sums, *Methylocella*, *Methylosinus* and *Methylobacter*, did not change significantly in abundance or order of highest contributor. We expected that a higher proportion of type II and *Verrucomicrobia* methanotrophs would contribute higher to the cumulative sums due to their ability to resist acidic conditions found in bog environments (Hakobyan and Liesack, 2020; Dedysh, 2002, 2009), and this was confirmed by our results. Both type II *Methylocella* and *Methylosinus* are well adapted to the cold and acidic conditions common in northern ombrotrophic peatlands. These physiological traits explain why type II *Alphaproteobacteria* were dominant over type I *Gammaproteobacteria* and this is consistent with other research conducted in ombrotrophic bogs (Hakobyan and Liesack, 2020; Chen et al., 2008; Dedysh, 2002, 2009). However, the presence of thermophilic and halophilic *Verrucomicrobia* and *Gammaproteobacteria* methanotrophs, while lower in abundance, were also detected in each category. This indicates a tolerance to the acid and cold conditions experienced within northern ombrotrophic peatlands. These results, similar to those observed in the methanogen community, indicate that the methanotroph community hold the ability to continue to oxidise CH_4 under alternate environmental conditions.

4.3.2 Functional genes

The functional gene composition of methanogens and methanotrophs does not hold a strong relationship to the magnitude of CH_4 flux, contrary to results found by Zhang et al. (2019) were the authors observed significant correlation between mcrA and CH_4 flux. However, Zhang et al. (2019) only targeted *mcrA* and *pmoA* when analysing their results, while our approach used a wider diversity of methanogenesis and methanotrophy related genes, which may have contributed to the observed difference. In our comparison, we observed small variations

https://doi.org/10.5194/bg-2021-353
Preprint. Discussion started: 12 January 2022

in the relative abundance of genes when compared between HFM, MFM and LFM. The NMDS analysis agreed with the PERMANOVA and displayed overlap between samples with a distinct lack of cluster separation. This result indicates that the composition and relative abundance of functional genes has little variation between HFM, MFM and LFM.

The top three genes that contributed the most to the dissimilarities between HFM, MFM and LFM were *mcrA*, *hdrA* and *coxL*. Both *mcrA* and *hdrA* genes act as key enzymes in the biological formation of CH_4 and these genes are shared across hydrogenotrophic, acetoclastic and methylotrophic methanogens. The *mcrA* catalyzes the conversion of methyl-coenzyme M and coenzyme B into CH_4 and the heterodisulfide of coenzyme M (HS-CoM) and coenzyme B (HS-CoB) (Scheller et al., 2010; Thauer, 2019). Subsequently, CoM and CoB must be reduced to regenerate the CoM-SH and CoB-SH thiols which are used as electron donors by *mcrA*, which is then catalyzed by *hdrA* (Scheller et al., 2010; Buan et al., 2011). Therefore, a co-dependence between *mcrA* and *hdrA* exists and this is essential for the biological formation of CH_4. Due to the close nature of the two genes, targeting transcripts of *hdrA* may be important in future research.

We assumed that the abundance of *mcrA* genes would be higher in HFM when compared to MFM and LFM in accordance with previous research (Franchini et al., 2015; Liebner et al., 2012). However, the opposite was discovered with the average relative abundances of *mcrA* lower in HFM when compared to MFM and LFM. This result is surprising, as previous research has found a significant relationship between key genes such as the *mcrA* and the magnitude of CH_4 flux (Freitag et al., 2010; Zhang et al., 2019). We believe that the analysis of *mcrA* transcripts, rather than gene abundance, would yield a stronger relationship to the CH_4 flux. While a close relationship of *mcrA* gene abundance to transcripts was observed by Franchini et al. (2015), gene abundance may not be the most effective in explaining small differences between flux categories. Rather, the use of gene transcripts may be a more appropriate method (Franchini et al., 2015; Freitag et al., 2010).

In addition to *mcrA* and *hdrA*, the presence of carbon monoxide (CO) dehydrogenase (*cooS*, *coxL*, *coxM*, *coxS*, *cutL*, *cutM*) was of particular interest. These genes code for CO dehydrogenase and are involved in the Acetyl-CoA pathway, which is not directly included in methanogenesis. Comparatively little is known today of the ecology, physiology, and biochemistry of CO utilization by methanogens (Ferry, 2010; Fischer et al., 1931). Only a few species are reported to metabolize CO, including *Methanosarcina*, which contributed 5% to 6% of the cumulative sums within our comparisons. However, according to Ferry (2010) it is not yet known if CO is a viable energy source for methanogens in peatland environments. Furthermore, the presence of six genes that code for

https://doi.org/10.5194/bg-2021-353
Preprint. Discussion started: 12 January 2022

539 CO dehydrogenase within the top 70% of cumulative sums indicates that if CO is a viable substrate, a high
540 functional potential could exist within peatland environments to use this lesser known substrate during
541 methanogenesis.

542 It is important to note that carbon monoxide dehydrogenase and *hdrA* genes are not strictly utilized by
543 methanogens. A wide variety of microbes, including *Acetogens*, sulfur oxidizing *Archaea* and *Bacteria*, utilize
544 the above-mentioned genes (Ernst et al., 2021; Ferry, 2010; Maupin-Furlow and Ferry, 1996). Therefore, the
545 distribution of how many genes are strictly related to methanogenesis can be difficult to determine.

546 **4.4 The relationship between microbial diversity and the magnitude of CH_4 flux**

547 The Shannon α-diversity of 2.38 indicates a low diversity. An et al. (2019), found that peatland environments hold
548 an average Shannon α-diversity index of 6.8. However, the lower diversity observed in our is most likely due to
549 the targeted approach, which only enriches taxa related to CH_4 metabolism. The targeted approach, combined
550 with the filtering of taxa that exclude other microbial groups, which if included within the analysis, would better
551 represent peatland environments.

552 Low dissimilarity was observed between the mesocosms when calculating the β- diversity. HFM held the highest
553 dissimilarity indicating that as the CH_4 flux increases, the abundance and variability of microbe's increase. As the
554 magnitude of CH_4 flux reduced, the abundance and variability of methanogens and methanotrophs decreased. This
555 trend indicates that β- diversity may act as a proxy for CH_4 emissions, contrary to results found by Zhang et al.
556 (2019) who concluded that abundance, rather than composition mainly affects CH_4 emissions. However, due to
557 the low replication in HFM and LFM, further research is needed to make this conclusion.

558 **4.5 $\delta^{13}C$ of emitted CH_4 and proportion of taxa**

559 The $\delta^{13}C$ analysis and presence of multiple hydrogenotrophic methanogens indicated that the dominant metabolic
560 pathway observed within the mesocosms was hydrogenotrophic methanogenesis. All flux categories returned the
561 $\delta^{13}C$ signal within the hydrogenotrophic range ($\delta^{13}C = -110‰$ to $-60‰$) (Chanton, 2005; Whiticar, 1999). This
562 is not a surprising result, as there appears to be a pattern in northern and temperate wetlands of increasing
563 hydrogenotrophic methanogenesis going from minerotrophic peats to ombrotrophic acidic bogs, similar to
564 conditions observed with our site (Galand et al., 2010; Holmes et al., 2015; Horn et al., 2003a). Furthermore, the

https://doi.org/10.5194/bg-2021-353
Preprint. Discussion started: 12 January 2022

positive correlation between $\delta^{13}C\text{-}CH_4$ to CH_4 emission rate indicates the CH_4 emission to be mostly controlled by the trophic status for methanogenesis, rather than methanotrophy (Hornibrook, 2009).

5.0 Conclusion

In this paper, we addressed differences in the composition of taxonomy and functional genes of CH_4 producing and consuming microbes between three flux categories: HFM, MFM and LFM. In addition, we determined that β-diversity increases in HFM when compared to the MFM and LFM categories, and we observed that the $\delta^{13}C$ of emitted CH_4 matches the dominant taxonomic functional group.

We observed small differences in the composition of both taxa and functional genes between flux categories. This indicates that, although we observe high spatial variability in CH_4 fluxes, we cannot explain this variability by taxonomic composition and functional genes alone. Interestingly, we observed that β-diversity was higher in HFM when compared to MFM and LFM – indicating that diversity may be a plausible proxy for CH_4 fluxes.

The dominant methanogen, *Methanoregula*, made up over 50% of the community composition. This, in combination with the remaining hydrogenotrophic methanogens observed within the community composition, matched the observed $\delta^{13}C$ isotopic signature of emitted CH_4. This indicates that the dominant metabolic pathway in the Fäjemyr peatland is hydrogenotrophic methanogenesis. However, the presence of acetoclastic and methylotrophic taxa plus type I, II and *Verrucomicrobia* methanotrophs indicates that the microbial community holds the ability to produce and consume CH_4 via alternate metabolic pathways. This is important in terms of future climate scenarios where peatlands can expect altered nutrient status, hydrology or peat chemistry. If this happens, we can expect that there will be methanogen and methanotrophs present to continue to produce and consume CH_4 due to the potential for alternate metabolic pathways.

Our results show that genetic potential is of minor importance in explaining small scale variability of CH_4 fluxes observed in peatland environments. Additional proxies to understand this variability may be found in gene expression studies where activity levels are better represented rather than genetic potential. With the modeling community working continuously to build robust predictions of peatland CH_4 emissions (Chadburn et al., 2020), the need for inclusion of genomic data may be considered. With this knowledge, the combination of traditional CH_4 drivers, metagenomics and metatranscriptomic studies could increase our understanding of how and at what rate the key CH_4 producing and consuming microorganisms' function in peatland ecosystems. This information

https://doi.org/10.5194/bg-2021-353
Preprint. Discussion started: 12 January 2022

592 on microbial diversity is necessary on both temporal and spatial scales for the development of more robust models
593 to accurately predict upcoming emissions under future climate scenarios.

594 **Data availability**

595 The annotated metagenomes are available at the MG-RAST server under the project ID: 91052. In addition, all
596 raw sequences will be made public via NCBI Bio Project ID: PRJNA691743 upon acceptance of this manuscript.

597 **Code availability**

598 Code used in the analysis can be found at https://github.com/joel332/Analysis-of-captured-metagenomic-
599 data/tree/main.

600 **Author contributions**

601 JW, LS and DA planned the experiment; JW, LS, JR performed the measurements; JW and VL analyzed the data,
602 JW wrote the draft; JW, LS, JR, VL an DA reviewed and edited the manuscript.

603 **Competing interests**

604 The authors declare that they have no conflict of interest.

605 **Acknowledgments**

606 We would like to thank Pia and the staff from the Centre for Genomic Research, Ulrika from Roche Diagnostics
607 Scandinavia, Frans-Jan Parmentier, colleagues, friends and family for the valuable discussions and Oskar Ström
608 for laboratory assistance. The data handling was enabled by resources in project (SNIC 2019/8-365) provided by
609 the Swedish National Infrastructure for Computing (SNIC) at UPPMAX, partially funded by the Swedish
610 Research Council through grant agreement no. 2018-05973.

611 **Financial support**

612 We would like to thank the Swedish research council for environment, agricultural sciences and spatial planning
613 (FORMAS - 997-610) and the Crafoord Institute (20200738) for financial support.

614 **References**

615 An, J., Liu, C., Wang, Q., Yao, M., Rui, J., Zhang, S., and Li, X.: Soil bacterial community
616 structure in Chinese wetlands, Geoderma, 337, 290-299,
617 https://doi.org/10.1016/j.geoderma.2018.09.035, 2019.

https://doi.org/10.5194/bg-2021-353
Preprint. Discussion started: 12 January 2022

618 Andersen, R., Chapman, S. J., and Artz, R. R. E.: Microbial communities in natural and
619 disturbed peatlands: A review, Soil Biology and Biochemistry, 57, 979-994,
620 https://doi.org/10.1016/j.soilbio.2012.10.003, 2013.
621 Anderson, M. J.: A new method for non-parametric multivariate analysis of variance, Austral
622 Ecology, 26, 32-46, 10.1046/j.1442-9993.2001.01070.x, 2001.
623 Bridgham, S. D., Cadillo-Quiroz, H., Keller, J. K., and Zhuang, Q.: Methane emissions from
624 wetlands: biogeochemical, microbial, and modeling perspectives from local to global scales,
625 Global Change Biology, 19, 1325-1346, https://doi.org/10.1111/gcb.12131, 2013.
626 Brumfield, K. D., Huq, A., Colwell, R. R., Olds, J. L., and Leddy, M. B.: Microbial resolution of
627 whole genome shotgun and 16S amplicon metagenomic sequencing using publicly available
628 NEON data, PLOS ONE, 15, e0228899, 10.1371/journal.pone.0228899, 2020.
629 Buan, N., Kulkarni, G., and Metcalf, W.: Chapter two - Genetic Methods for Methanosarcina
630 Species, in: Methods in Enzymology, edited by: Rosenzweig, A. C., and Ragsdale, S. W.,
631 Academic Press, 23-42, https://doi.org/10.1016/B978-0-12-385112-3.00002-0, 2011.
632 Chadburn, S. E., Aalto, T., Aurela, M., Baldocchi, D., Biasi, C., Boike, J., Burke, E. J.,
633 Comyn-Platt, E., Dolman, A. J., Duran-Rojas, C., Fan, Y., Friborg, T., Gao, Y., Gedney, N.,
634 Göckede, M., Hayman, G. D., Holl, D., Hugelius, G., Kutzbach, L., Lee, H., Lohila, A.,
635 Parmentier, F.-J. W., Sachs, T., Shurpali, N. J., and Westermann, S.: Modeled Microbial
636 Dynamics Explain the Apparent Temperature Sensitivity of Wetland Methane Emissions,
637 Global Biogeochemical Cycles, 34, e2020GB006678,
638 https://doi.org/10.1029/2020GB006678, 2020.
639 Chanton, J. P., Chaser, L. C., Glaser, P. & Siegel, D: Stable Isotopes and Biosphere-
640 Atmosphere Interactions. [Elektronisk resurs] Processes and Biological Controls,
641 Physiological Ecology series, Elsevier2005.
642 Chen, Y., Dumont, M. G., Murrell, J. C., McNamara, N. P., Chamberlain, P. M., Bodrossy, L.,
643 and Stralis-Pavese, N.: Diversity of the active methanotrophic community in acidic peatlands
644 as assessed by mRNA and SIP-PLFA analyses, Environmental microbiology, 10, 446-459,
645 10.1111/j.1462-2920.2007.01466.x, 2008.
646 Chroňáková, A., Bárta, J., Kaštovská, E., Urbanová, Z., and Picek, T.: Spatial heterogeneity
647 of belowground microbial communities linked to peatland microhabitats with different plant
648 dominants, FEMS microbiology ecology, 95, 10.1093/femsec/fiz130, 2019.
649 Crill, P. M., Bartlett, K. B., Harriss, R. C., Gorham, E., Verry, E. S., Sebacher, D. I., Madzar,
650 L., and Sanner, W.: Methane flux from Minnesota Peatlands, Global Biogeochemical Cycles,
651 2, 371-384, 10.1029/GB002i004p00371, 1988.
652 Dean, J. F., Middelburg, J. J., Röckmann, T., Aerts, R., Blauw, L. G., Egger, M., Jetten, M.
653 S. M., Jong, A. E. E., Meisel, O. H., Rasigraf, O., Slomp, C. P., Zandt, M. H., and Dolman, A.
654 J.: Methane Feedbacks to the Global Climate System in a Warmer World, Reviews of
655 Geophysics, 56, 207-250, doi:10.1002/2017RG000559, 2018.
656 Dedysh, S. N.: Methanotrophic Bacteria of Acidic Sphagnum Peat Bogs, Microbiology, 71,
657 638-650, 10.1023/A:1021467520274, 2002.
658 Dedysh, S. N.: Exploring methanotroph diversity in acidic northern wetlands: Molecular and
659 cultivation-based studies, Microbiology, 78, 655-669, 10.1134/s0026261709060010, 2009.
660 Dinsdale, E. A., Edwards, R. A., Hall, D., Angly, F., Breitbart, M., Brulc, J. M., Furlan, M.,
661 Desnues, C., Haynes, M., Li, L., McDaniel, L., Moran, M. A., Nelson, K. E., Nilsson, C.,
662 Olson, R., Paul, J., Brito, B. R., Ruan, Y., Swan, B. K., Stevens, R., Valentine, D. L.,
663 Thurber, R. V., Wegley, L., White, B. A., and Rohwer, F.: Functional metagenomic profiling
664 of nine biomes, Nature, 452, 629-632, 10.1038/nature06810, 2008.
665 Dlugokencky, E. J., Houweling, S., Bruhwiler, L., Masarie, K. A., Lang, P. M., Miller, J. B.,
666 and Tans, P. P.: Atmospheric methane levels off: Temporary pause or a new steady-state?,
667 Geophysical Research Letters, 30, https://doi.org/10.1029/2003GL018126, 2003.
668 Dlugokencky, E. J., Bruhwiler, L., White, J. W. C., Emmons, L. K., Novelli, P. C., Montzka, S.
669 A., Masarie, K. A., Lang, P. M., Crotwell, A. M., Miller, J. B., and Gatti, L. V.: Observational
670 constraints on recent increases in the atmospheric CH4 burden, Geophysical Research
671 Letters, 36, https://doi.org/10.1029/2009GL039780, 2009.

https://doi.org/10.5194/bg-2021-353
Preprint. Discussion started: 12 January 2022

672 Ernst, C., Kayastha, K., Koch, T., Venceslau, S. S., Pereira, I. A. C., Demmer, U., Ermler, U.,
673 and Dahl, C.: Structural and spectroscopic characterization of a HdrA-like subunit from
674 Hyphomicrobium denitrificans, The FEBS Journal, 288, 1664-1678,
675 https://doi.org/10.1111/febs.15505, 2021.
676 Escobar-Zepeda, A., Vera-Ponce de León, A., and Sanchez-Flores, A.: The Road to
677 Metagenomics: From Microbiology to DNA Sequencing Technologies and Bioinformatics,
678 Frontiers in Genetics, 6, 10.3389/fgene.2015.00348, 2015.
679 Ferry, J. G.: Enzymology of one-carbon metabolism in methanogenic pathways, FEMS
680 Microbiology Reviews, 23, 13-38, doi:10.1111/j.1574-6976.1999.tb00390.x, 1999.
681 Ferry, J. G.: CO in methanogenesis, Annals of Microbiology, 60, 1-12, 10.1007/s13213-009-
682 0008-5, 2010.
683 Fierer, N., Barberán, A., and Laughlin, D. C.: Seeing the forest for the genes: using
684 metagenomics to infer the aggregated traits of microbial communities, Frontiers in
685 Microbiology, 5, 10.3389/fmicb.2014.00614, 2014.
686 Fischer, F., Lieske, R., and Winzer, K.: Die umsetzungen des kohlenoxyds, Biochem. Z, 236,
687 247-267, 1931.
688 Franchini, A. G., Henneberger, R., Aeppli, M., and Zeyer, J.: Methane dynamics in an alpine
689 fen: a field-based study on methanogenic and methanotrophic microbial communities, FEMS
690 microbiology ecology, 91, 10.1093/femsec/fiu032, 2015.
691 Freitag, T. E., Toet, S., Ineson, P., and Prosser, J. I.: Links between methane flux and
692 transcriptional activities of methanogens and methane oxidizers in a blanket peat bog, FEMS
693 microbiology ecology, 73, 157-165, 10.1111/j.1574-6941.2010.00871.x, 2010.
694 Galand, P. E., Fritze, H., and Yrjala, K.: Microsite-dependent changes in methanogenic
695 populations in a boreal oligotrophic fen, Environmental microbiology, 5, 1133-1143, 2003.
696 Galand, P. E., Yrjälä, K., and Conrad, R.: Stable carbon isotope fractionation during
697 methanogenesis in three boreal peatland ecosystems, Biogeosciences, 7, 3893-3900,
698 10.5194/bg-7-3893-2010, 2010.
699 Galand, P. E., Fritze, H., Conrad, R., and Yrjälä, K.: Pathways for Methanogenesis and
700 Diversity of Methanogenic Archaea in Three Boreal Peatland Ecosystems, Applied and
701 environmental microbiology, 71, 2195-2198, doi:10.1128/AEM.71.4.2195-2198.2005, 2005.
702 Galand, P. E., Saarnio, S., Fritze, H., and Yrjälä, K.: Depth related diversity of methanogen
703 Archaea in Finnish oligotrophic fen, FEMS microbiology ecology, 42, 441-449,
704 10.1111/j.1574-6941.2002.tb01033.x, 2002.
705 Gasc, C., Peyretaillade, E., and Peyret, P.: Sequence capture by hybridization to explore
706 modern and ancient genomic diversity in model and nonmodel organisms, Nucleic acids
707 research, 44, 4504-4518, 10.1093/nar/gkw309, 2016.
708 Gravel, D., Bell, T., Barbera, C., Combe, M., Pommier, T., and Mouquet, N.: Phylogenetic
709 constraints on ecosystem functioning, Nature Communications, 3, 1117,
710 10.1038/ncomms2123, 2012.
711 Hadley, W.: Ggplot2: Elegant Graphics for Data Analysis, Springer2016.
712 Hakobyan, A. and Liesack, W.: Unexpected metabolic versatility among type II
713 methanotrophs in the Alphaproteobacteria, Biological Chemistry, 401, 1469-1477,
714 doi:10.1515/hsz-2020-0200, 2020.
715 He, S., Malfatti, S. A., McFarland, J. W., Anderson, F. E., Pati, A., Huntemann, M.,
716 Tremblay, J., Rio, T. G. d., Waldrop, M. P., Windham-Myers, L., Tringe, S. G., and Bailey, M.
717 J.: Patterns in Wetland Microbial Community Composition and Functional Gene Repertoire
718 Associated with Methane Emissions, mBio, 6, e00066-00015, doi:10.1128/mBio.00066-15,
719 2015.
720 Herv, M.: RVAideMemoire: Testing and Plotting Procedures for Biostatistics, 2021.
721 Holm, S.: A Simple Sequentially Rejective Multiple Test Procedure, Scandinavian Journal of
722 Statistics, 6, 65-70, 1979.
723 Holmes, M. E., Chanton, J. P., Tfaily, M. M., and Ogram, A.: CO2 and CH4 isotope
724 compositions and production pathways in a tropical peatland, Global Biogeochemical
725 Cycles, 29, 1-18, https://doi.org/10.1002/2014GB004951, 2015.

https://doi.org/10.5194/bg-2021-353
Preprint. Discussion started: 12 January 2022

Horn, M. A., Matthies, C., Küsel, K., Schramm, A., and Drake, H. L.: Hydrogenotrophic methanogenesis by moderately acid-tolerant methanogens of a methane-emitting acidic peat, Applied and environmental microbiology, 69, 74-83, 10.1128/aem.69.1.74-83.2003, 2003a.
Horn, M. A., Matthies, C., Küsel, K., Schramm, A., and Drake, H. L.: Hydrogenotrophic Methanogenesis by Moderately Acid-Tolerant Methanogens of a Methane-Emitting Acidic Peat, Applied and environmental microbiology, 69, 74-83, doi:10.1128/AEM.69.1.74-83.2003, 2003b.
Hornibrook, E. R. C.: The stable carbon isotope composition of methane produced and emitted from northern peatlands, Washington DC American Geophysical Union Geophysical Monograph Series, 184, 187, 10.1029/2008gm000828, 2009.
Hothorn, T., Winell, H., Hornik, K., A van de Wiel, M., and Zeileis, A.: Conditional Inference Procedures in a Permutation Test Framework, CRAN, 1.4-2, 2021.
Joabsson, A., Christensen, T. R., and Wallén, B.: Vascular plant controls on methane emissions from northern peatforming wetlands, Trends in Ecology & Evolution, 14, 385-388, https://doi.org/10.1016/S0169-5347(99)01649-3, 1999.
Sickle: A sliding-window, adaptive, quality-based trimming tool for FastQ files (Version 1.33): https://github.com/najoshi/sickle, last access: 19-2-2020.
Juottonen, H., Tuittila, E.-S., Juutinen, S., Fritze, H., and Yrjälä, K.: Seasonality of rDNA- and rRNA-derived archaeal communities and methanogenic potential in a boreal mire, The ISME journal, 2, 1157-1168, 10.1038/ismej.2008.66, 2008.
Kanehisa, M., Sato, Y., Kawashima, M., Furumichi, M., and Tanabe, M.: KEGG as a reference resource for gene and protein annotation, Nucleic Acids Research, 44, D457-D462, 10.1093/nar/gkv1070, 2015.
Keane, J. B., Toet, S., Ineson, P., Weslien, P., Stockdale, J. E., and Klemedtsson, L.: Carbon Dioxide and Methane Flux Response and Recovery From Drought in a Hemiboreal Ombrotrophic Fen, Frontiers in Earth Science, 8, 10.3389/feart.2020.562401, 2021.
Keeling, C. D.: The concentration and isotopic abundances of atmospheric carbon dioxide in rural areas, Geochimica et Cosmochimica Acta, 13, 322-334, 10.1016/0016-7037(58)90033-4, 1958.
Korrensalo, A., Männistö, E., Alekseychik, P., Mammarella, I., Rinne, J., Vesala, T., and Tuittila, E. S.: Small spatial variability in methane emission measured from a wet patterned boreal bog, Biogeosciences, 15, 1749-1761, 10.5194/bg-15-1749-2018, 2018.
Kushwaha, S. K., Manoharan, L., Meerupati, T., Hedlund, K., and Ahren, D.: MetCap: a bioinformatics probe design pipeline for large-scale targeted metagenomics, BMC bioinformatics, 16, 65, 10.1186/s12859-015-0501-8, 2015.
Lane, D., Pace, B., Olsen, G., Stahl, D., and Sogin, M.: Rapid determination of 16S ribosomal RNA sequences for phylogenetic analyses, Proceedings of the National Academy of Sciences, 83, 4972, 1986.
Liebner, S., Schwarzenbach, S. P., and Zeyer, J.: Methane emissions from an alpine fen in central Switzerland, Biogeochemistry, 109, 287-299, 10.1007/s10533-011-9629-4, 2012.
Lin, X., Green, S., Tfaily, M. M., Prakash, O., Konstantinidis, K. T., Corbett, J. E., Chanton, J. P., Cooper, W. T., and Kostka, J. E.: Microbial Community Structure and Activity Linked to Contrasting Biogeochemical Gradients in Bog and Fen Environments of the Glacial Lake Agassiz Peatland, Applied and environmental microbiology, 78, 7023-7031, 10.1128/aem.01750-12, 2012.
Lin, X., Tfaily, M. M., Green, S. J., Steinweg, J. M., Chanton, P., Imvittaya, A., Chanton, J. P., Cooper, W., Schadt, C., and Kostka, J. E.: Microbial metabolic potential for carbon degradation and nutrient (nitrogen and phosphorus) acquisition in an ombrotrophic peatland, Applied and environmental microbiology, 80, 3531-3540, 10.1128/AEM.00206-14, 2014.
Livingston, G. and Hutchinson, G.: Enclosure-based measurement of trace gas exchange: applications and sources of error, Biogenic trace gases: measuring emissions from soil and water, 51, 14-51, 1995.
Lonnstad, J. and Löfroth, M.: Myskyddsplan för Sverige, Naturvårdsverket, Stockholm, Sweden, 1994.

https://doi.org/10.5194/bg-2021-353
Preprint. Discussion started: 12 January 2022

781 Lund, M., Lindroth, A., Christensen, T. R., and Ström, L.: Annual CO2 balance of a
782 temperate bog, Tellus B, 59, 804-811, 10.1111/j.1600-0889.2007.00303.x, 2007.
783 Manoharan, L., Kushwaha, S. K., Ahrén, D., and Hedlund, K.: Agricultural land use
784 determines functional genetic diversity of soil microbial communities, Soil Biology and
785 Biochemistry, 115, 423-432, https://doi.org/10.1016/j.soilbio.2017.09.011, 2017.
786 Manoharan, L., Kushwaha, S. K., Hedlund, K., and Ahren, D.: Captured metagenomics:
787 large-scale targeting of genes based on 'sequence capture' reveals functional diversity in
788 soils, DNA research : an international journal for rapid publication of reports on genes and
789 genomes, 22, 451-460, 10.1093/dnares/dsv026, 2015.
790 Martin, M.: Cutadapt removes adapter sequences from high-throughput sequencing reads,
791 2011, 17, 3, 10.14806/ej.17.1.200, 2011.
792 Mastepanov, M., Sigsgaard, C., Tagesson, T., Ström, L., Tamstorf, M. P., Lund, M., and
793 Christensen, T. R.: Revisiting factors controlling methane emissions from high-Arctic tundra,
794 Biogeosciences, 10, 5139-5158, 10.5194/bg-10-5139-2013, 2013.
795 Maupin-Furlow, J. A. and Ferry, J. G.: Analysis of the CO dehydrogenase/acetyl-coenzyme
796 A synthase operon of Methanosarcina thermophila, Journal of Bacteriology, 178, 6849-6856,
797 10.1128/jb.178.23.6849-6856.1996, 1996.
798 Meyer, F., Paarmann, D., D'Souza, M., Olson, R., Glass, E. M., Kubal, M., Paczian, T.,
799 Rodriguez, A., Stevens, R., Wilke, A., Wilkening, J., and Edwards, R. A.: The metagenomics
800 RAST server – a public resource for the automatic phylogenetic and functional analysis of
801 metagenomes, BMC bioinformatics, 9, 386, 10.1186/1471-2105-9-386, 2008.
802 O'Leary, N. A., Wright, M. W., Brister, J. R., Ciufo, S., Haddad, D., McVeigh, R., Rajput, B.,
803 Robbertse, B., Smith-White, B., Ako-Adjei, D., Astashyn, A., Badretdin, A., Bao, Y., Blinkova,
804 O., Brover, V., Chetvernin, V., Choi, J., Cox, E., Ermolaeva, O., Farrell, C. M., Goldfarb, T.,
805 Gupta, T., Haft, D., Hatcher, E., Hlavina, W., Joardar, V. S., Kodali, V. K., Li, W., Maglott, D.,
806 Masterson, P., McGarvey, K. M., Murphy, M. R., O'Neill, K., Pujar, S., Rangwala, S. H.,
807 Rausch, D., Riddick, L. D., Schoch, C., Shkeda, A., Storz, S. S., Sun, H., Thibaud-Nissen,
808 F., Tolstoy, I., Tully, R. E., Vatsan, A. R., Wallin, C., Webb, D., Wu, W., Landrum, M. J.,
809 Kimchi, A., Tatusova, T., DiCuccio, M., Kitts, P., Murphy, T. D., and Pruitt, K. D.: Reference
810 sequence (RefSeq) database at NCBI: current status, taxonomic expansion, and functional
811 annotation, Nucleic Acids Res, 44, D733-745, 10.1093/nar/gkv1189, 2016.
812 Oksanen, J., Blanchet, F. G., Friendly, M., Kindt, R., Legendre, P., McGlinn, D., Minchin, P.
813 R., O'Hara, R. B., Simpson, G. L., Solymos, P., Henry, M., Stevens, H., Szoecs, E., and
814 Wagner, H.: vegan: Community Ecology Package, 2019.
815 Pereira-Marques, J., Hout, A., Ferreira, R. M., Weber, M., Pinto-Ribeiro, I., van Doorn, L.-J.,
816 Knetsch, C. W., and Figueiredo, C.: Impact of Host DNA and Sequencing Depth on the
817 Taxonomic Resolution of Whole Metagenome Sequencing for Microbiome Analysis,
818 Frontiers in Microbiology, 10, 10.3389/fmicb.2019.01277, 2019.
819 Preston, M., Smemo, K., McLaughlin, J., and Basiliko, N.: Peatland Microbial Communities
820 and Decomposition Processes in the James Bay Lowlands, Canada, Frontiers in
821 Microbiology, 3, 10.3389/fmicb.2012.00070, 2012.
822 Saunois, M., Jackson, R. B., Bousquet, P., Poulter, B., and Canadell, J. G.: The growing role
823 of methane in anthropogenic climate change, Environmental Research Letters, 11, 120207,
824 10.1088/1748-9326/11/12/120207, 2016a.
825 Saunois, M., Bousquet, P., Poulter, B., Peregon, A., Ciais, P., Canadell, J. G., Dlugokencky,
826 E. J., Etiope, G., Bastviken, D., Houweling, S., Janssens-Maenhout, G., Tubiello, F. N.,
827 Castaldi, S., Jackson, R. B., Alexe, M., Arora, V. K., Beerling, D. J., Bergamaschi, P., Blake,
828 D. R., Brailsford, G., Brovkin, V., Bruhwiler, L., Crevoisier, C., Crill, P., Covey, K., Curry, C.,
829 Frankenberg, C., Gedney, N., Hoeglund-Isaksson, L., Ishizawa, M., Ito, A., Joos, F., Kim, H.-
830 S., Kleinen, T., Krummel, P., Lamarque, J.-F., Langenfelds, R., Locatelli, R., Machida, T.,
831 Maksyutov, S., McDonald, K. C., Marshall, J., Melton, J. R., Morino, I., Naik, V., Odoherty,
832 S., Parmentier, F.-J. W., Patra, P. K., Peng, C., Peng, S., Peters, G. P., Pison, I., Prigent, C.,
833 Prinn, R., Ramonet, M., Riley, W. J., Saito, M., Santini, M., Schroeder, R., Simpson, I. J.,
834 Spahni, R., Steele, P., Takizawa, A., Thornton, B. F., Tian, H., Tohjima, Y., Viovy, N.,
835 Voulgarakis, A., van Weele, M., van der Werf, G. R., Weiss, R., Wiedinmyer, C., Wilton, D.

https://doi.org/10.5194/bg-2021-353
Preprint. Discussion started: 12 January 2022

836 J., Wiltshire, A., Worthy, D., Wunch, D., Xu, X., Yoshida, Y., Zhang, B., Zhang, Z., and Zhu,
837 Q.: The global methane budget 2000-2012, Earth System Science Data, 8, 697-751,
838 10.5194/essd-8-697-2016, 2016b.
839 Saunois, M., Stavert, A. R., Poulter, B., Bousquet, P., Canadell, J. G., Jackson, R. B.,
840 Raymond, P. A., Dlugokencky, E. J., Houweling, S., Patra, P. K., Ciais, P., Arora, V. K.,
841 Bastviken, D., Bergamaschi, P., Blake, D. R., Brailsford, G., Bruhwiler, L., Carlson, K. M.,
842 Carrol, M., Castaldi, S., Chandra, N., Crevoisier, C., Crill, P. M., Covey, K., Curry, C. L.,
843 Etiope, G., Frankenberg, C., Gedney, N., Hegglin, M. I., Höglund-Isaksson, L., Hugelius, G.,
844 Ishizawa, M., Ito, A., Janssens-Maenhout, G., Jensen, K. M., Joos, F., Kleinen, T., Krummel,
845 P. B., Langenfelds, R. L., Laruelle, G. G., Liu, L., Machida, T., Maksyutov, S., McDonald, K.
846 C., McNorton, J., Miller, P. A., Melton, J. R., Morino, I., Müller, J., Murguia-Flores, F., Naik,
847 V., Niwa, Y., Noce, S., O'Doherty, S., Parker, R. J., Peng, C., Peng, S., Peters, G. P.,
848 Prigent, C., Prinn, R., Ramonet, M., Regnier, P., Riley, W. J., Rosentreter, J. A., Segers, A.,
849 Simpson, I. J., Shi, H., Smith, S. J., Steele, L. P., Thornton, B. F., Tian, H., Tohjima, Y.,
850 Tubiello, F. N., Tsuruta, A., Viovy, N., Voulgarakis, A., Weber, T. S., van Weele, M., van der
851 Werf, G. R., Weiss, R. F., Worthy, D., Wunch, D., Yin, Y., Yoshida, Y., Zhang, W., Zhang, Z.,
852 Zhao, Y., Zheng, B., Zhu, Q., Zhu, Q., and Zhuang, Q.: The Global Methane Budget 2000–
853 2017, Earth Syst. Sci. Data, 12, 1561-1623, 10.5194/essd-12-1561-2020, 2020.
854 Scheller, S., Goenrich, M., Boecher, R., Thauer, R. K., and Jaun, B.: The key nickel enzyme
855 of methanogenesis catalyses the anaerobic oxidation of methane, Nature, 465, 606-608,
856 10.1038/nature09015, 2010.
857 SMHI: Klimat i förändring. En jämförelse av temperatur och nederbörd 1991-2005 med
858 1961-1990. , Swedish Meteorological anf Hydrological Institute, Norrköping, Sweden, 2006.
859 Strack, M., Waddington, J. M., and Tuittila, E. S.: Effect of water table drawdown on northern
860 peatland methane dynamics: Implications for climate change, Global Biogeochemical
861 Cycles, 18, doi:10.1029/2003GB002209, 2004.
862 Ström, L., Tagesson, T., Mastepanov, M., and Christensen, T. R.: Presence of Eriophorum
863 scheuchzeri enhances substrate availability and methane emission in an Arctic wetland, Soil
864 Biology and Biochemistry, 45, 61-70, https://doi.org/10.1016/j.soilbio.2011.09.005, 2012.
865 Ström, L., Falk, J. M., Skov, K., Jackowicz-Korczynski, M., Mastepanov, M., Christensen, T.
866 R., Lund, M., and Schmidt, N. M.: Controls of spatial and temporal variability in CH4 flux in a
867 high arctic fen over three years, Biogeochemistry, 125, 21-35, 10.1007/s10533-015-0109-0,
868 2015.
869 Sun, L., Song, C., Miao, Y., Qiao, T., and Gong, C.: Temporal and spatial variability of
870 methane emissions in a northern temperate marsh, Atmospheric Environment, 81, 356-363,
871 10.1016/j.atmosenv.2013.09.033, 2013.
872 Thauer, R. K.: Methyl (Alkyl)-Coenzyme M Reductases: Nickel F-430-Containing Enzymes
873 Involved in Anaerobic Methane Formation and in Anaerobic Oxidation of Methane or of Short
874 Chain Alkanes, Biochemistry, 58, 5198-5220, 10.1021/acs.biochem.9b00164, 2019.
875 Thom, M., Bösinger, R., Schmidt, M., and Levin, I.: The regional budget of atmospheric
876 methane of a highly populated area, Chemosphere, 26, 143-160,
877 https://doi.org/10.1016/0045-6535(93)90418-5, 1993.
878 Tveit, A., Schwacke, R., Svenning, M. M., and Urich, T.: Organic carbon transformations in
879 high-Arctic peat soils: key functions and microorganisms, The ISME journal, 7, 299-311,
880 10.1038/ismej.2012.99, 2013.
881 Ungerer, M. C., Johnson, L. C., and Herman, M. A.: Ecological genomics: understanding
882 gene and genome function in the natural environment, Heredity, 100, 178-183,
883 10.1038/sj.hdy.6800992, 2008.
884 Wania, R., Ross, I., and Prentice, I. C.: Integrating peatlands and permafrost into a dynamic
885 global vegetation model: 2. Evaluation and sensitivity of vegetation and carbon cycle
886 processes, Global Biogeochemical Cycles, 23, doi:10.1029/2008GB003413, 2009.
887 Wania, R., Ross, I., and Prentice, I. C.: Implementation and evaluation of a new methane
888 model within a dynamic global vegetation model: LPJ-WHyMe v1.3.1, Geosci. Model Dev.,
889 3, 565-584, 10.5194/gmd-3-565-2010, 2010.

https://doi.org/10.5194/bg-2021-353
Preprint. Discussion started: 12 January 2022

890 Ward, D. M., Cohan, F. M., Bhaya, D., Heidelberg, J. F., Kühl, M., and Grossman, A.:
891 Genomics, environmental genomics and the issue of microbial species, Heredity, 100, 207-
892 219, 10.1038/sj.hdy.6801011, 2008.
893 Warton, D. I., Wright, S. T., and Wang, Y.: Distance-based multivariate analyses confound
894 location and dispersion effects, Methods in Ecology and Evolution, 3, 89-101,
895 https://doi.org/10.1111/j.2041-210X.2011.00127.x, 2012.
896 Wei, T. and Simko, V.: R package "corrplot": Visualization of a Correlation Matrix, 2017.
897 Wendlandt, K.-D., Stottmeister, U., Helm, J., Soltmann, B., Jechorek, M., and Beck, M.: The
898 potential of methane-oxidizing bacteria for applications in environmental biotechnology,
899 Engineering in Life Sciences, 10, 87-102, https://doi.org/10.1002/elsc.200900093, 2010.
900 Whiticar, M. J.: Carbon and hydrogen isotope systematics of bacterial formation and
901 oxidation of methane, Chemical Geology, 161, 291-314, 10.1016/S0009-2541(99)00092-3,
902 1999.
903 Zhang, Y., Cui, M., Duan, J., Zhuang, X., Zhuang, G., and Ma, A.: Abundance, rather than
904 composition, of methane-cycling microbes mainly affects methane emissions from different
905 vegetation soils in the Zoige alpine wetland, MicrobiologyOpen, 8, e00699,
906 10.1002/mbo3.699, 2019.
907